Report 3695

NAVAL SHIP RESEARCH AND DEVELOPMENT CENTER

Bethesda, Maryland 20034

ADDED MASS AND DAMPING COEFFICIENTS OF HEAVING TWIN CYLINDERS IN A FREE SURFACE

ADDED MASS AND DAMPING COEFFICIENTS OF HEAVING TWIN CYLINDERS IN A FREE SURFACE

by

C. M. Lee, H. Jones, and J. W. Bedel

APPROVED FOR PUBLIC RELEASE: DISTRIBUTION UNLIMITED

SHIP PERFORMANCE DEPARTMENT
RESEARCH AND DEVELOPMENT REPORT

August 1971

Report 3695

The Naval Ship Research and Development Center is a U. S. Navy center for laboratory effort directed at achieving improved sea and air vehicles. It was formed in March 1967 by merging the David Taylor Model Basin at Carderock, Maryland with the Marine Engineering Laboratory at Annapolis, Maryland. The Mine Defense Laboratory (now Naval Ship R & D Laboratory) Panama City, Florida became part of the Center in November 1967.

Naval Ship Research and Development Center

Bethesda, Md. 20034

MAJOR NSRDC ORGANIZATIONAL COMPONENTS

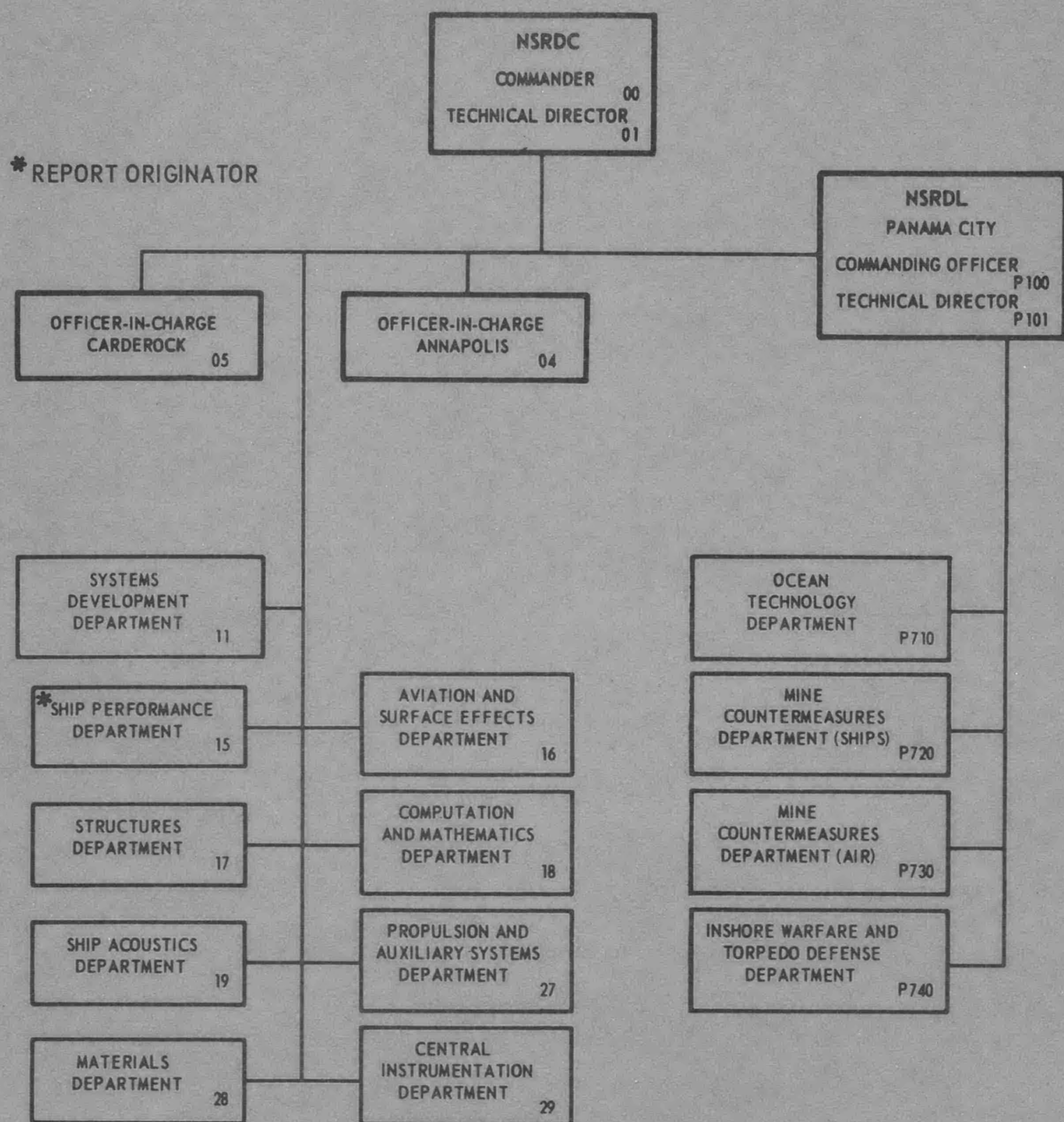

NDW-NSRDC 3960/43 (3-70)

NDW-NSRDC 3960/44 (REV. 8/71)

GPO 917-872

DEPARTMENT OF THE NAVY
NAVAL SHIP RESEARCH AND DEVELOPMENT CENTER
BETHESDA, MD. 20034

ADDED MASS AND DAMPING COEFFICIENTS OF HEAVING TWIN CYLINDERS IN A FREE SURFACE

by
C. M. Lee, H. Jones, and J. W. Bedel

August 1971

Report 3695

TABLE OF CONTENTS

LIST OF FIGURES

LIST OF FIGURES (CONT.)

NOTATION

a	Half-beam of cylinder
b	Separation distance (see Figure 1)
c_j	jth line segment of cylinder contour
F	Vertical hydrodynamic force
G	Complex wave source near a vertical wall
g	Gravitational acceleration
h_o	Amplitude of oscillation
k	Spring constant
K	σ^2/g
M	Displaced mass of twin cylinders
$\underline{n}$	Unit normal vector on the surface of cylinder pointing into the fluid
Q_j	Source strength at jth segment
s_j	(ξ_j, η_j) – Lefthand end point of jth line segment
z	$x + iy$
α_j	Tangent angle of the jth line segment
δ	$\sigma^2 a/g = Ka$
ζ	$\xi + i\eta$
λ	Damping
$\bar{\lambda}$	Damping coefficient formed by dividing the damping λ by the product of the displaced fluid mass and the radian frequency
μ	Added mass
$\bar{\mu}$	Added mass coefficient formed by dividing the added mass μ by the fluid mass displaced by twin cylinders
ρ	Density of fluid
σ	Radian frequency of oscillation
Φ	Velocity potential function of harmonic time dependence
ϕ	$(=\phi_c + j\,\phi_s)$ steady velocity potential of complex function with respect to $j = \sqrt{-1}$
ϕ_c	The real part of ϕ; subscript c indicates that it is associated with $\cos \sigma t$
ϕ_s	The imaginary of ϕ; subscript s indicates that it is associated with $\sin \sigma t$

ABSTRACT

A potential flow problem, dealing with twin horizontal cylinders of arbitrary cross sectional forms vertically oscillating in a free surface is investigated. An associated experiment is carried out for four different sets of twin cylinders. The results from the theory and the experiment are compared and are found in good agreement.

ADMINISTRATIVE INFORMATION

The theoretical part of this work was authorized by the Naval Material Command under the in-house research project and was funded under Project R01101, Task ZR011 0101. The experimental part was funded under the Naval Ship Systems Command Research, Development, Test and Evaluation program, General Hydromechanics Research, Subproject S-R009 01 01, Task 0100.

INTRODUCTION

Investigations conducted in the past, concerning the motion of ships in waves, have demonstrated the practicability of the strip theory for obtaining the hydrodynamic forces and moments acting on ships in waves. The present work provides the means for computing the hydrodynamic coefficients associated with the motion of catamarans in regular head waves. Since the strip method is to be applied in obtaining the necessary hydrodynamic coefficients, the basic problem is reduced to a two-dimensional flow problem.

Many investigators have already studied similar problems. Potash[1] obtained a solution without providing numerical results for semisubmerged twin circular cylinders, rigidly connected from above, heaving in a free surface. Ohkusu[2] investigated the same problem as Potash and obtained the values of added mass and damping for various frequencies and separation distances between the two cylinders. Later, Ohkusu[3] studied two or more rigidly connected cylinders heaving, swaying, or rolling and applied the results obtained from this investigation to the motions of multihull ships in waves. He used an approximate scheme utilizing the results of his previous work[2] on the twin semicircular cylinders to obtain the added masses and dampings of the noncircular cross sections of the ship. Wang and Wahab[4] also investigated theoretically and experimentally the problem of twin semicircular cylinders heaving in a free surface. They showed excellent agreement between their theoretical and experimental results;

[1] References are listed on page 48.

de Jong[5] derived solutions without providing numerical results for heaving, swaying, or rolling twin cylinders of symmetric cross sections, using conformal mapping.

The previously discussed investigators used the method of multipole expansion to determine the unknown velocity potential. This method was first introduced by Ursell[6] in the solution of the problem of a semicircular cylinder heaving in a free surface. Ursell's method assumed a series of singularities of increasing order placed at the intersections of the midplane of each cylinder with the free-surface plane, with each of the singularities independently satisfying the free-surface boundary condition. The unknown coefficients of the series were obtained by satisfying the kinematic boundary condition on the cylinder surface. In principle, this method may be applied to any shape that can be mapped from a circle. However, the investigators cited previously chose only those cylinders which were symmetric about their own vertical midplanes.

The present investigation deals with twin cylinders of arbitrary cross sections which do not have to be symmetric about their own vertical midplanes. (The problem still assumes the two cylinders to be of identical shape.) The mathematical tool adopted in solving the problem is the method of source distribution on the cross sectional contours of both cylinders. The same method was applied for an oscillating single cylinder by Frank[7].

Since the heaving twin cylinders constitute a symmetric flow about a vertical midplane, the problem can be reduced to the case of a single cylinder heaving near a vertical wall. In fact, the problem is treated in this fashion.

Tests for four different shapes of twin cylinders were performed by vertically oscillating the twin cylinders in a calm free surface. The four cross sectional forms chosen were shaped as a semicircle, rectangle, a right triangle, and an isosceles triangle. Several separation distances between the two cylinders were chosen, and the oscillation frequencies were selected to cover the practical range of catamaran motions in waves. The results from the theory and the experiment were compared and were found in good agreement.

THEORY

FORMULATION

Two semisubmerged identical horizontal cylinders of infinite length, connected above the waterline, are vertically oscillated in a calm water surface with an amplitude which is small compared to the beam of the cylinders. The fluid in which the cylinders are immersed is assumed incompressible; its motion, irrotational; and its depth, infinite. It is also assumed that the oscillation has been going on long enough for the initial transient effect of the fluid to be completely phased out.

The x-axis is taken to coincide with the undisturbed free surface and the y-axis is directed vertically upward. The origin is taken at the midpoint between the two cylinders.

The distance from the origin to each half point of the cylinder beam is taken to be b; the cylinder beam is taken to be 2a; see Figure 1. Since the problem described previously dictates an obvious hydrodynamic symmetry about the y-axis, the problem can be reduced to the right half of the plane only.

By introducing a velocity potential function Φ (x,y,t) and by properly prescribing the necessary conditions on the fluid boundaries, a boundary-value problem in terms of Φ can be formulated. With the assumption of small oscillation, only the linear frequency response of the fluid to the disturbance will be considered. Thus the velocity potential can be written as

$$\Phi(x, y, t) = \mathrm{Re}_j \left\{\phi(x,y)e^{-j\sigma t}\right\} = \phi_c \cos \sigma t + \phi_s \sin \sigma t \qquad (1)$$

where

$$\phi = \phi_c + j\phi_s \qquad (2)$$

The motion of any point on the surface of the cylinder is expressed by

$$y(t) = h_o \sin \sigma t \qquad (3)$$

Continuity of mass implies that

$$\nabla^2 \phi(x, y) = 0 \qquad (4)$$

in the fluid region.

The assumption of a slight disturbance on the free surface leads to a linearized form of the free-surface condition, which is given in the form of*

$$\phi_y(x, 0) - K\phi = 0 \qquad (5)$$

where $K = \sigma^2/g$. The derivation of the expression is given in Wehausen and Laitone[8].

The linearized kinematic condition on the cylinder contour is given by

$$\phi_n = \nabla\phi \cdot \underline{n} = V_n \qquad (6)$$

at the mean position of the cylinder. Here $\underline{n}$ is an outward unit normal vector on the cylinder contour, and V_n is the normal component of the velocity of the cylinder contour. It can be readily shown that

*When the space variables x and y and the time variable t are used as subscript, they indicate partial derivatives.

$$V_n = h_o \sigma \cos(n,y) \tag{7}$$

where cos (n,y) means the directional cosine between the normal vector and the y direction.

Due to the symmetry of the fluid disturbance about the y-axis, there cannot be flow crossing the y-axis. That is,

$$\phi_x(0,y) = 0 \tag{8}$$

This condition implies that the plane x=0 can be regarded as a rigid wall.

The expected decay of the fluid disturbance as $y \to -\infty$ can be described by

$$\nabla \phi(x,-\infty)=0 \tag{9}$$

The far-field behavior of ϕ as $x \to \infty$ should represent outgoing waves, i.e., Sommerfeld's radiation condition,

$$\lim_{x \to \infty} (\phi_x - jK\phi) = 0 \tag{10}$$

This completes the statement of our problem, and the boundary conditions are shown in Figure 2. The solution of this boundary-value problem will provide the sought hydrodynamic quantities such as pressure distribution, hydrodynamic force, added mass, and damping coefficients.

SOLUTION

The solution of the velocity potential $\phi(x,y)$ is assumed to be represented by a distribution of source singularities over the immersed contour of the cylinder; see Reference 9.

$$\phi(p) = \int_{c_o} Q(s) G_R(p;s)\, ds \tag{11}$$

where $p = (x, y)$ is the field point,

$Q = Q_c + jQ_s$ is source density,

$G_R = G_{Rc} + j\, G_{Rs}$ is the source, and

c_o is the immersed contour of the cylinder in $y<0$.

A source of unit strength below a free surface can be expressed in the form of

$$G_R(x,y;\xi,\eta) = \log r_1 + H(x,y;\xi,\eta) \tag{12}$$

where $r_1 = [(x-\xi)^2+(y-\eta)^2]^{1/2}$, (ξ,η) is the point of the location of the source, and $\nabla^2 H=0$ everywhere in $y<0$. It is further required that G_R satisfy the free-surface condition

$$G_{R_y}(x,0)-KG_R=0$$

the radiation condition

$$\lim_{x \to \infty} (G_{Rx} - jKG_R) = 0$$

and the deepwater condition

$$\nabla G_R(x,-\infty)=0$$

The solution for G_R is given, for example, in Reference 8 in terms of a complex velocity potential $G(z;\zeta)$ which is defined by

$$\begin{aligned} G(z;\zeta) &= G_R(x,y;\xi,\eta) + i\,G_I(x,y;\xi,\eta) \\ &= \frac{1}{2\pi}\Big\{\log(z-\zeta) - \log(z-\bar{\zeta}) \\ &\quad + 2\,⨍_0^{\infty} \frac{e^{-ik(z-\bar{\zeta})}}{K-k}\,dk - j2\pi e^{-iK(z-\bar{\zeta})}\Big\} \end{aligned} \tag{13}$$

Here $⨍_0^{\infty}$ indicates a principal value integral, and $\bar{\zeta} = \xi - i\eta$.

It is desired to have the function G_R satisfy the symmetric condition

$$G_{R\,x}(0,y;\xi,\eta)=0$$

By use of the well-known reflection principle, G_R can be made to satisfy the previously shown symmetric condition. That is, if a new function is formed by

$$F(z;\zeta) = G(z;\zeta) + G(z;-\bar{\zeta}) \tag{14}$$

it can be shown that

$$\mathrm{Re}_i \left\{ \frac{d}{dz} F(0+i\,y;\zeta) \right\} = 0$$

Thus, by adding the term $G(z;-\bar{\zeta})$ to the right-hand side of Equation (13), the function G is redefined as

$$G(z;\zeta) = G_R(x,y;\xi,\eta) + i\,G_I = G_{Rc} + j\,G_{Rs} + i\,(G_{Ic} + jG_{Is})$$

$$= \frac{1}{2\pi}\Big\{\log\frac{(z-\zeta)(z+\bar{\zeta})}{(z-\bar{\zeta})(z+\zeta)} + 2\int_0^\infty \frac{e^{-ik(z-\bar{\zeta})} + e^{-ik(z+\zeta)}}{K-k}\,dk$$

$$-j2\pi\,(e^{-iK(z-\bar{\zeta})} + e^{-iK(z+\zeta)})\Big\} \qquad (15)$$

The function G_R given in Equation (15) satisfies the same boundary conditions as imposed on ϕ, except for the kinematic boundary condition on the cylinder contour. This remaining boundary condition is used to obtain the strengths of the sources Q(s) given in Equation (11).

It will be assumed that the contour of the cylinder c_o can be approximated by N number of straight-line segments, each of which is denoted by c_j, $j = 1, 2, \cdots, N$. Thus, Equation (11) can be written as

$$\phi(p) = \sum_{j=1}^{N} \int_{c_j} Q(s)\,G_R(p;s)\,ds$$

it will be assumed further that the variation of source strength on each segment is so small that it can be treated as constant on each segment. The latter assumption yields the expression

$$\phi(p) = \sum_{j=1}^{N} Q_j \int_{c_j} G_R(p;s)\,ds \qquad (16)$$

When the kinematic boundary condition given by Equation (6) is applied on Equation (16) it follows that

$$\phi_n(p_o) = \sum_{j=1}^{N} Q_j\,(\underline{n}\cdot\nabla)\int_{c_j} G_R(p;s)\,ds\,\Big|_{p=p_o}$$

$$= h_o\,\sigma\cos\alpha \qquad (17)$$

where α is the tangent angle of the contour of the cylinder at the point p_o. By taking N number of points on the contour c_o and by assuming that these points are located at the midpoints of the line segments c_j (Figure 3), it can be shown that

$$\sum_{j=1}^{N} Q_j\,(\underline{n}\cdot\nabla)\int_{c_j} G_R(p;s)\,ds\,\Big|_{p=p_i\epsilon c_o} = h_o\,\sigma\cos\alpha_i \qquad (18)$$

for $i = 1, 2, \cdots, N$

By definition the function Q and G are made of real and imaginary parts with respect to the complex number $j = \sqrt{-1}$. Thus, the separation of the real and the imaginary parts of Equation (20) yields

$$\sum_{j=1}^{N} Q_{c_j} I_{ij} - \sum_{j=1}^{N} Q_{s_j} J_{ij} = h_o \sigma \cos \alpha_i$$

$$\sum_{j=1}^{N} Q_{c_j} J_{ij} + \sum_{j=1}^{N} Q_{s_j} I_{ij} = 0 \qquad (19)$$

for $i = 1, 2, \cdots, N$,

where

$$I_{ij} = (\underline{n} \cdot \nabla) \int_{C_j} G_{Rc}\,(p; s)\, ds \Big|_{p = p_i \epsilon c_o} \qquad (20)$$

$$J_{ij} = (\underline{n} \cdot \nabla) \int_{C_j} G_{Rs}\,(p; s)\, ds \Big|_{p = p_i \epsilon c_o} \qquad (21)$$

and the derivation of these matrix coefficients is given in Appendix A. Equation (19) represents 2N simultaneous equations from which the unknown coefficients Q_{cj}, Q_{sj}, $j = 1, 2, \cdots, N$, can be obtained.

ADDED MASS AND DAMPING

The hydrodynamic pressure at the point (x_o, y_o) on the cylinder is obtained from the linearized Bernoulli equation by

$$\begin{aligned} P(x_o, y_o, t) &= -\rho \Phi_t\,(x_o, y_o, t) \\ &= -\rho \mathrm{Re}_j \left\{ -j\, \sigma\, \phi\,(x_o, y_o)\, e^{-j\sigma t} \right\} \\ &= -\rho\sigma\,(\phi_s \cos \sigma t - \phi_c \sin \sigma t) \end{aligned} \qquad (22)$$

The vertical hydrodynamic force acting on the twin cylinders can be obtained by

$$\begin{aligned} F &= -2 \int_{c_o} P \cos \alpha\, ds \\ &= 2\rho\sigma\,(\cos \sigma t \int_{c_o} \phi_s \cos \alpha\, ds - \sin \sigma t \int_{c_o} \phi_c \cos \alpha\, ds) \end{aligned} \qquad (23)$$

The separation of Equation (16) into the real and the imaginary parts yields

$$\phi_c(x_o, y_o) = \sum_{j=1}^{N} \Big(Q_{cj} \int_{C_j} G_{Rc}\,(x_o, y_o; s)\,ds - Q_{sj} \int_{C_j} G_{Rs}\,(x_o, y_o; s)\,ds\Big) \qquad (24)$$

and

$$\phi_s(x_o, y_o) = \sum_{j=1}^{N} \Big(Q_{cj} \int_{C_j} G_{Rs}\,(x_o, y_o; s)\,ds + Q_{sj} \int_{C_j} G_{Rc}\,(x_o, y_o; s)\,ds\Big) \qquad (25)$$

where G_{Rc} and G_{Rs} can be obtained from Equation (15). The integrals $\int_{C_j} G_{Rc}\,ds$ and $\int_{C_j} G_{Rs}\,ds$ are evaluated in Appendix B.

If we let the total hydrodynamic force be expressed in the form

$$F = -\mu\ddot{y}\,(t) - \lambda\dot{y}, \qquad (26)$$

we have by substitution of $y(t) = h_o \sin \sigma t$

$$F = h_o \sigma^2 \mu \sin \sigma t - h_o \sigma\lambda \cos \sigma t \qquad (27)$$

By equating Equations (23) and (27), we find that

$$\text{Added Mass} = \mu = -\frac{2\rho}{h_o \sigma} \int_{C_o} \phi_c \cos \alpha ds$$

$$= \frac{-2\rho}{h_o \sigma} \sum_{j,k=1}^{N} (Q_{cj} A_{jk} - Q_{sj} B_{jk}) \cos \alpha_k \left| \Delta S_k \right| \qquad (28)$$

$$\text{Damping} = \lambda = \frac{2\rho}{h_o} \int_{C_o} \phi_s \cos \alpha ds$$

$$= \frac{-2\rho}{h_o} \sum_{j,k=1}^{N} (Q_{cj} B_{jk} + Q_{sj} A_{jk}) \cos \alpha_k \left| \Delta S_k \right| \qquad (29)$$

where

$$\left|\Delta S_k\right| = \left|S_{k+1} - S_k\right| = [(\xi_{k+1} - \xi_k)^2 + (\eta_{k+1} - \eta_k)^2]^{1/2}$$

$$A_{jk} = \int_{C_j} G_{Rc}\,(x_k, y_k; s)\,ds \tag{30}$$

$$B_{jk} = \int_{C_j} G_{Rs}\,(x_k, y_k; s)\,ds \tag{31}$$

EXPERIMENT

EXPERIMENTAL SETUP

Cylindrical-type models, each consisting of two wooden hulls 7.5 ft in length, were tested to determine their heave added masses and damping coefficients. The twin-hull configurations with their dimensions are shown in Table 1 along with the hull separations (b-to-a ratios) which were tested for each set. The dimensions b and a are indicated on the twin-cylinder model in Figure 1. The tests were conducted in two series, the first was concerned with the semicircular cylinders, and the second comprised the remaining cylinders, including some repeated tests on the semicircular cylinders for checking purposes.

In order to approach the desired two-dimensional case, a piece of one-half inch plywood (3 x 7.5 ft) was attached vertically to each of the twin-hull configurations. This also served as rigid coupling between the hulls. Except for the tests of the semicircular cylinders for b/a = 2, 3, and 4, to minimize oscillation of these end boards and to improve rigidity, the boards were reinforced with aluminum angles on the outside as shown in Figure 4. The angles were mounted with head bolts countersunk through the boards into tapped holes in the angles to minimize forces which might result from adding the angles. Also shown in Figure 4 with the complete model setup is the X-frame, used for attachment to the oscillator.

For measuring the force required to oscillate the model, four ±100-lb block gages were used to obtain most of the data for the semicircular cylinders, while ±25 lb block gages, one at each end of the cylinders, were used for other cylinders.

The heaving frequency of the model was dependent upon the voltage input to the oscillator motor. This allowed essentially any frequency to be run within the desired range from 0.5 to 3.0 cps.

Two heave amplitudes were used during the tests. Generally the smaller amplitude of 0.25 in. was used at the higher frequencies, while the 0.50-in. amplitude was used at the lower end of the frequency range. In the midfrequency range, tests were made at both amplitudes to check linearity of the forces with the motion. As a further linearity check for the triangular

Table 1 - Figure Index of Added Mass and Damping Coefficients for Each Model Shape; Model Dimensions are Given in Inches

MODEL	a	COEF.	b/a 1.5	b/a 2	b/a 3	b/a 4
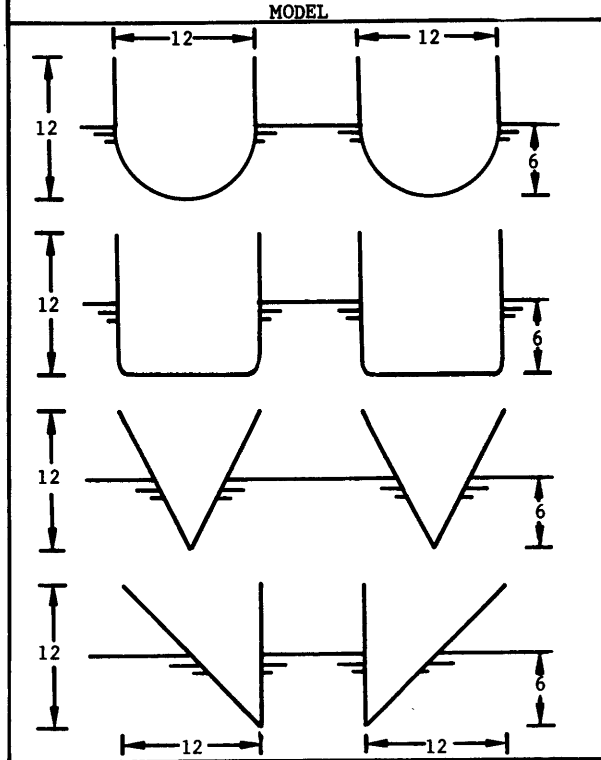	6	$\bar{\mu}$	Figure 7	Figure 8	Figure 9	Figure 10
		$\bar{\lambda}$	Figure 11	Figure 12	Figure 13	Figure 14
	6	$\bar{\mu}$	—	Figure 15	Figure 16	Figure 17
		$\bar{\lambda}$	—	Figure 18	Figure 19	Figure 20
	3	$\bar{\mu}$	—	—	Figure 21	Figure 22
		$\bar{\lambda}$	—	—	Figure 23	Figure 24
	3	$\bar{\mu}$	—	—	Figure 25	Figure 26
		$\bar{\lambda}$	—	—	Figure 27	Figure 28

models, tests were made over the midfrequency range at an amplitude of 0.75 in. The range of frequencies tested at each amplitude was extended to provide additional checks in some cases.

The tests were conducted at zero speed on Carriage 2 with the carriage at the mid-station of the center deep water basin. The plywood ends were parallel to the length of the basin. This was to prevent the waves generated by the oscillating model from being reflected back onto the model. Sufficient time was allowed between tests for the water to calm completely as an additional precaution against undue forces on the model.

EVALUATION OF DATA

To determine the hydrodynamic forces acting on each configuration heaving on the water surface, a harmonic heaving motion was imposed on the model floating on the surface. The equation of motion in this case is

$$(M + \mu)\,\ddot{x} + \lambda\dot{x} + kx = F(t)$$

where F(t) is the force needed to impose the prescribed motion

$x = h_o \sin \sigma t$ is the prescribed motion

M is displaced mass of the model

μ is added mass

λ is the damping factor

k is the spring constant

When data were being analyzed, it was assumed that the effect of the end boards on the added mass and damping of the cylinders could be neglected.

To obtain the added mass and damping, the forcing function was reduced to its fundamental components, which were in phase and 90 deg. out of phase with the displacement motion. This put the forcing function in the form

$$F(t) = A \sin \sigma t + B \cos \sigma t$$

Taking the first and second derivatives of x and equating the coefficients of like terms, the added mass and damping become

$$\mu = \frac{h_o k - A}{h_o \sigma^2} - M$$

$$\lambda = \frac{B}{h_o \sigma}$$

The spring constant k was calculated by taking the product of the waterplane area of the model and the specific weight of water. This was assumed constant over the range of amplitudes tested.

The previously described force coefficients A and B were obtained by analyzing the data in analog form during testing, using the electronic setup shown in Figure 5 for the first series of tests and Figure 6 for the second series of tests. This was done in the first case by summing two of the force signals and multiplying by 2 and in the second case by summing the four force signals and multiplying the sum by $\sin \sigma t$ and by $\cos \sigma t$, then integrating over the run time T. The result was multiplied by 2/T to determine the A and B coefficients as follows.

$$A = \frac{2}{T} \int_0^T F(t) \sin \sigma t \, dt$$

$$B = \frac{2}{T} \int_0^T F(t) \cos \sigma t \, dt$$

The total run time was taken during 30 heave cycles. The sine and cosine signals used for this analog Fourier analysis were obtained from a potentiometer which was mechanically coupled to the oscillator.

For the first series of tests with the circular cylinders the data were also reduced digitally. The reduction was accomplished during testing by first recording the force and motion signals in analog form on magnetic tape for the post-test analysis of the data. The data were then filtered, digitized, and fed to a computer program to determine the Fourier transform coefficients of the fundamental signals. The components in phase and 90 deg. out of phase with the displacement motion were derived from these coefficients.

RESULTS AND DISCUSSION

The added masses and the dampings obtained from the theory and the experiment are shown together for the purpose of comparison in Figures 7 through 28. The nondimensional parameters used in the graphs are

$\bar{\mu}$ = added mass coefficient $= \dfrac{\mu}{M}$

$\bar{\lambda}$ = damping coefficient $= \dfrac{\lambda}{M\sigma}$

δ = frequency number $= \dfrac{\sigma^2 a}{g}$

The difference between the two experimental data, one obtained by the analog method and the other by the digital method, was insignificant. The experimental results shown are mostly from the analog method. The experimental data for the semicircular cylinder are identical to those presented in Reference 4.

As mentioned earlier the theoretical approach to the solution of the problem employed in this work differs from the one employed in Reference 4 in which only semicircular cylinders were investigated. Thus, both theoretical results are also shown for the case of the semicircular cylinders. Except in the low frequency range and at some frequencies at which hydrodynamic discontinuity occurs, both results are in good agreement.

The results of the linearity check with the different amplitudes of oscillation show that the linear relation between the forcing motion and the resulting hydrodynamic force is valid for the semicircular and rectangular cylinders. But for the triangular cylinders, particularly for the isosceles triangular cylinders, the results from the different amplitudes show some disagreement in the low frequency range. The previously described fact suggests that nonlinear hydrodynamic effect could be caused by the sloping sides of the cylinders. Cylinders having sloped sides may create more free-surface disturbances than the wall-sided cylinders at lower frequencies so that the assumption of slight fluid disturbance to support the linearity relation may no longer be true for these cylinders at lower frequencies.

The nonsolid symbols shown in the results for the circular cylinders are the experimental data obtained with the end boards without the reinforcing angles.

Except for some discrepancies in the damping coefficients in the very low frequency range, both theoretical and experimental results are in good agreement.

At certain frequencies, the source distribution method used in solving an oscillating body problem causes a mathematical discontinuity. These frequencies, called irregular or critical, were first pointed out by John.[10] Frank[7] gave an approximate method for calculating these critical frequencies in terms of the beam-to-draft ratios of the cylinder. The approximate method equally applies for twin cylinders. The irregular behavior of the theoretical results at the critical frequencies is not shown in the figures. Smooth connections of the curves are made at the critical frequencies. A more satisfactory method of eliminating the critical frequencies is being investigated further. The mathematical proof for possible elimination of the critical frequencies has been established, and the computational implementation of the elimination technique still remains to be achieved.
tain frequencies in the solution of the twin-cylinder oscillation problem. These frequencies closely correspond to the gravity wavelength for deep water which satisfies the following relation

$$n \times (\text{wavelength}) = 2\,(b - a) \text{ for } n = 1, 2 \cdots \tag{32}$$

In terms of a frequency number, the relation becomes

$$\delta = \frac{n\pi}{(b/a-1)} \tag{32a}$$

The situation described previously is analogous to the breakdown of a periodic solution at certain frequencies for the problem of a wavemaker in a finite rectangular tank. The breakdown of the solution occurs when the relation given by Equation (32) is satisfied in which (b−a) corresponds to the length of the tank. In this work the y-axis can be regarded as a rigid wall, and the wavemaker is situated at a distance (b−a) from the wall. Both theoretical and experimental results prove that Equation (32a) provides fairly accurate values of the "resonance"* frequencies. The breakdown of the solution at these resonance frequencies may be prevented by seeking a time-dependent nonperiodic solution. However, we shall not attempt to do this here.

Large negative added masses are obtained in the low-frequency range for all four cylinders, except the experimental results for the right triangular cylinders. For heaving two-dimensional single bodies in a free surface, no negative heave added mass has been reported. Thus, the existence of negative added mass for twin cylinders strongly suggests the effect of hydrodynamic interaction between the two cylinders.

*This terminology is used to distinguish from the "critical" frequencies discussed earlier.

CONCLUDING REMARKS

1. Good agreement of the theoretical results with the experimental results confirms the validity of theory developed in this work.

2. The abrupt discontinuity of the results at certain frequencies found in the theory is also indicated by the experiment. The frequencies at which the discontinuity occurs, termed the resonance frequencies, are given by $\sigma_o = \sqrt{n\pi g/(b-a)}$ for $n=1, 2, \cdots$

3. The linearity between the forcing motion and the hydrodynamic force for the entire frequency range is confirmed for the twin cylinders having vertical sides, i.e., the semicircular and rectangular cylinders. With the exception of low frequencies, this linearity is also indicated for the twin cylinders having sloped sides, i.e., the triangular cylinders.

4. The variation of the values of added mass and damping is greater at lower frequencies ($\delta < 1$) than at higher frequencies. For the range of separation distance considered in this work, the numerical results indicate that as the frequency approaches infinity, the mutual hydrodynamic interaction between the two cylinders disappears.

5. The decrease of the separation distance between two cylinders results in (1) an increase of the lowest value of the resonance frequency, and (2) an increase of the absolute value of the negative added mass coefficient.

6. The validation of the theory found in this work for the case of heaving oscillation suggests extension of the theory to the cases of swaying and rolling oscillations.

ACKNOWLEDGMENTS

The authors would like to acknowledge the incorporation in this report of valuable suggestions rendered by Messrs. J. B. Hadler and V. J. Monacella.

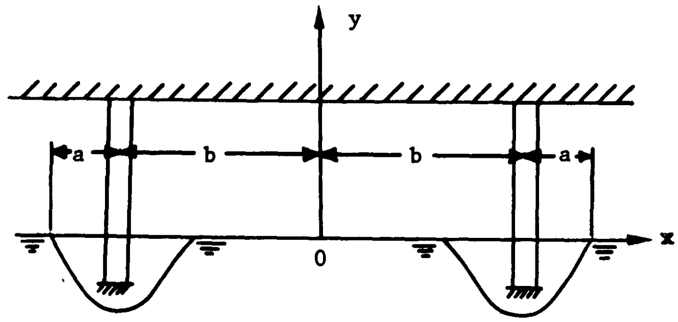

Figure 1 - Description of Coordinate System

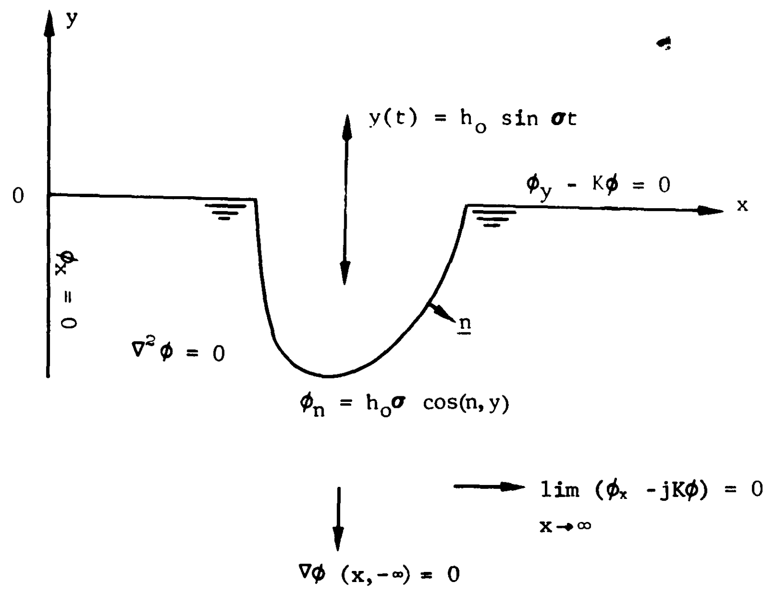

Figure 2 - Description of Boundary-Value Problem for $\phi(x, y)$

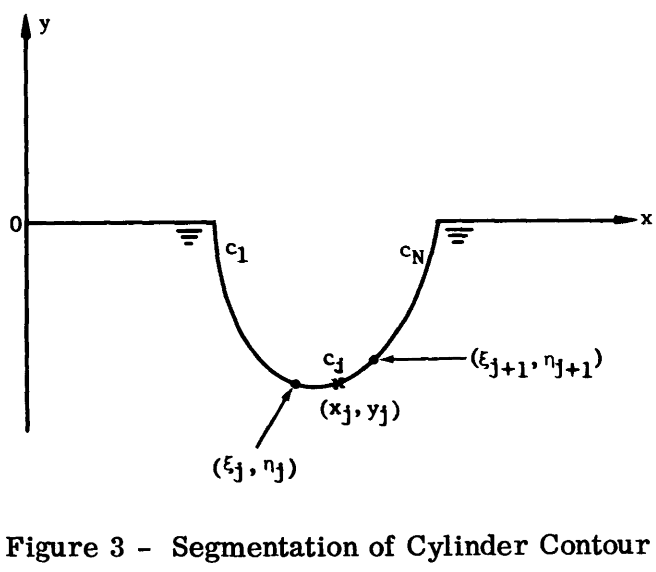

Figure 3 - Segmentation of Cylinder Contour

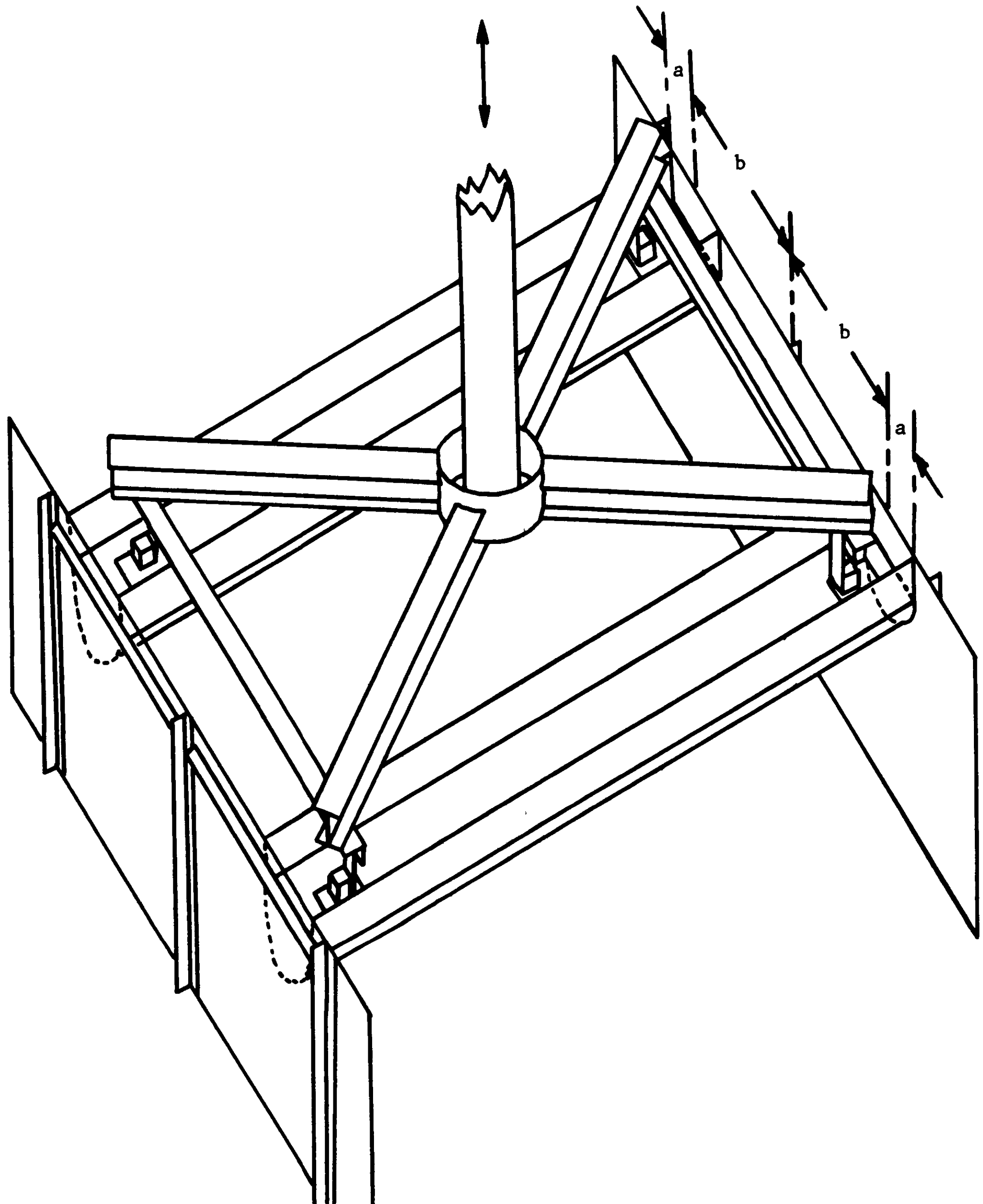

Figure 4 - Complete Model Setup for Testing

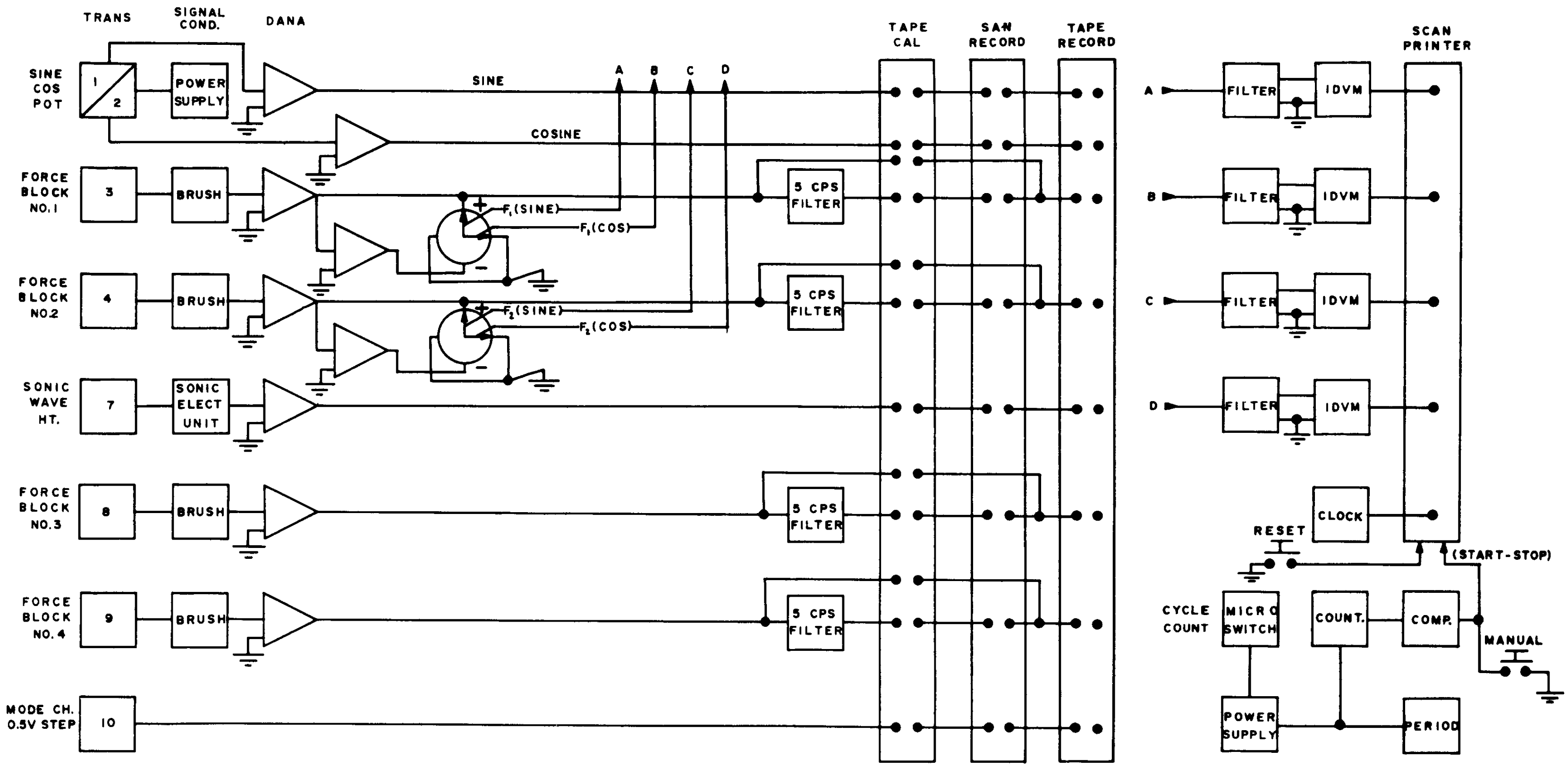

Figure 5 - Block Diagram of Electric Setup on Carriage 2 for First Series of Tests

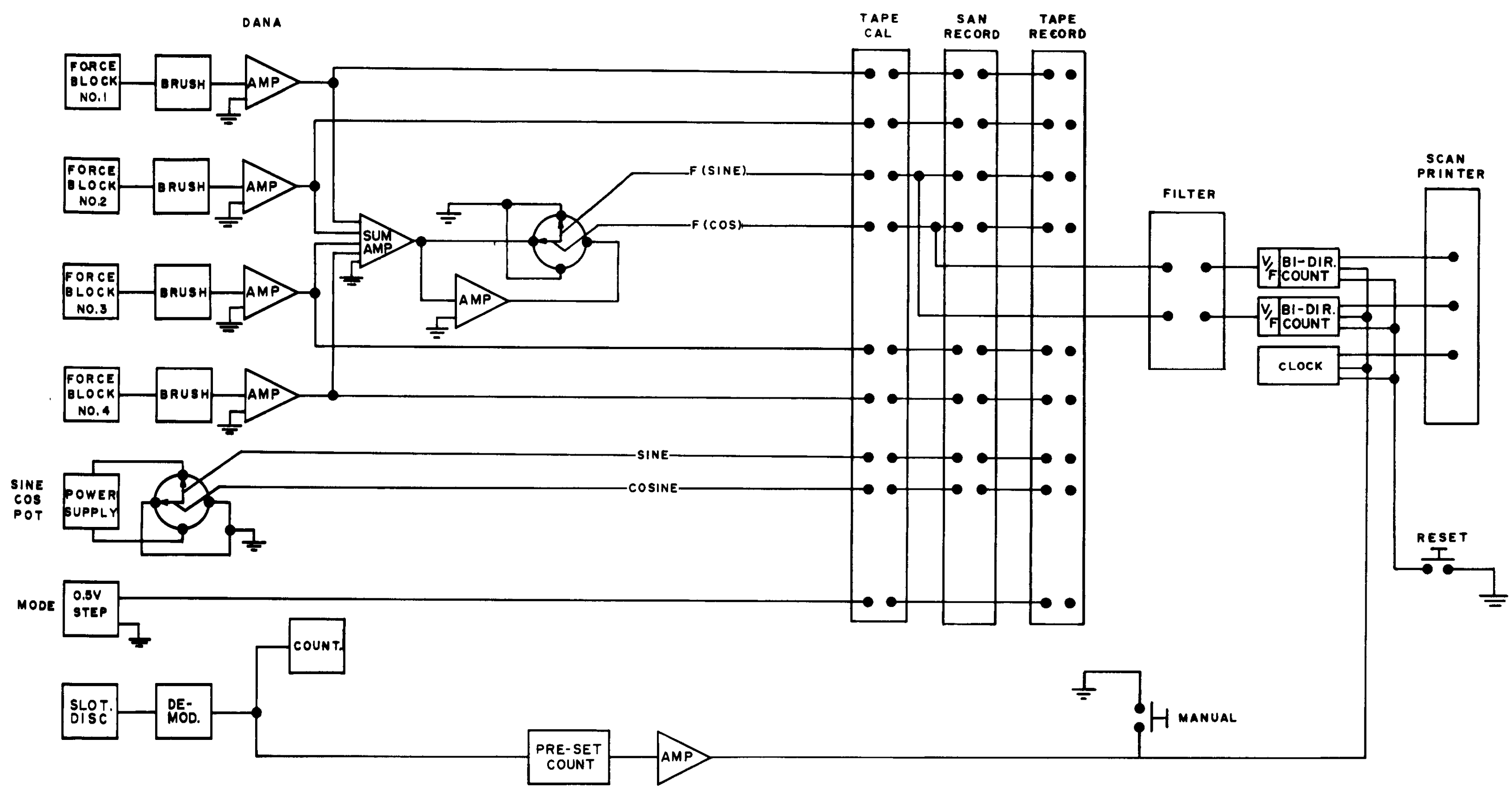

Figure 6 - Block Diagram of Electric Setup on Carriage 2 for Second Series of Tests

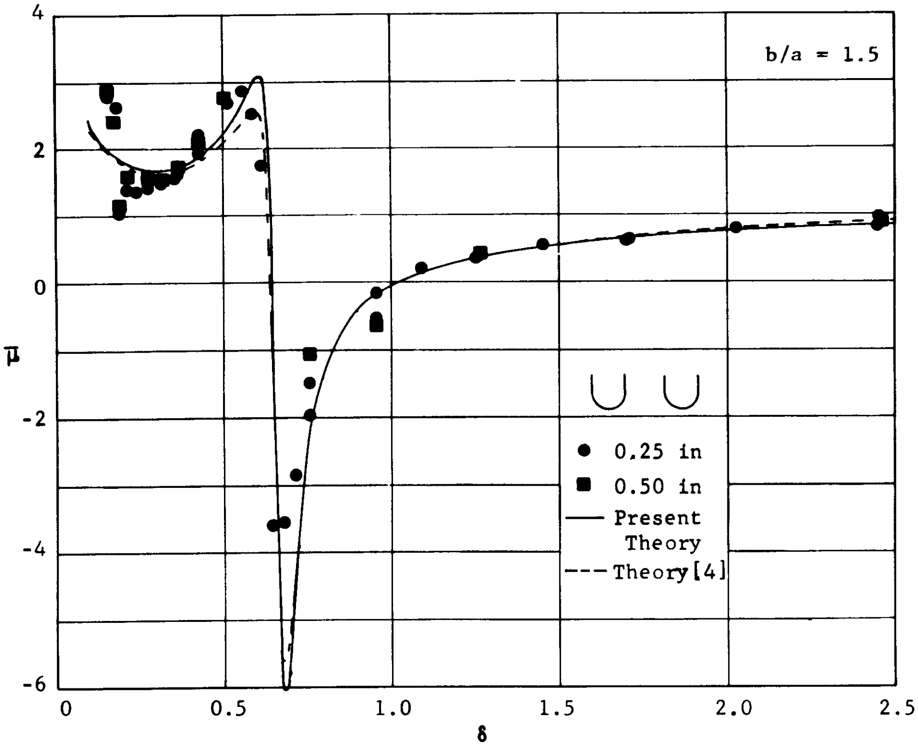

Figure 7 - Added Mass Coefficient versus Frequency Number for Twin Semicircular Cylinders for b/a=1.5

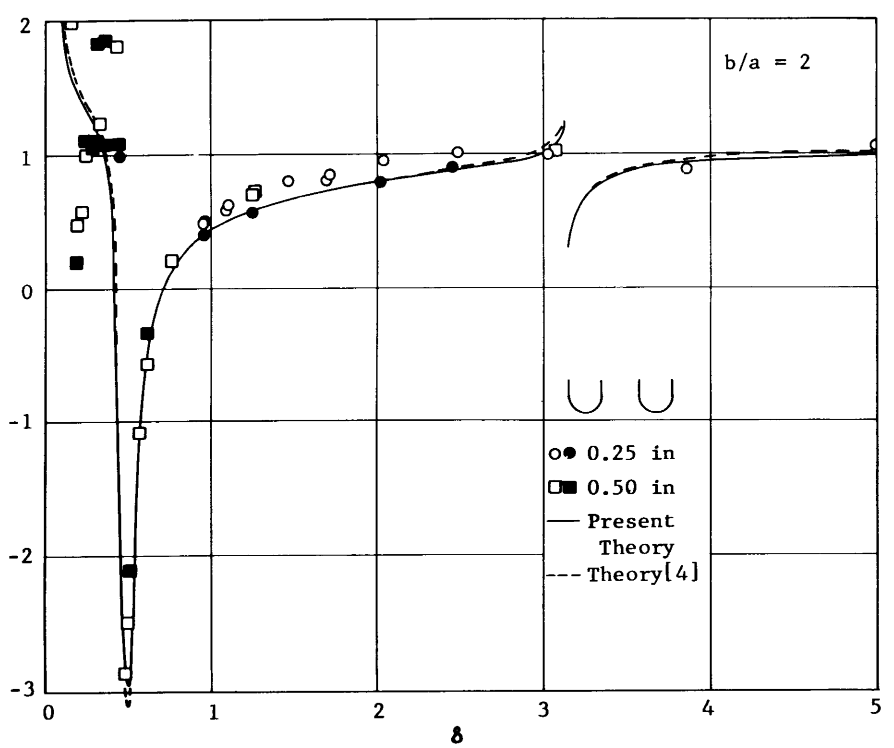

Figure 8 - Added Mass Coefficient versus Frequency Number for Twin Semicircular Cylinders for b/a=2

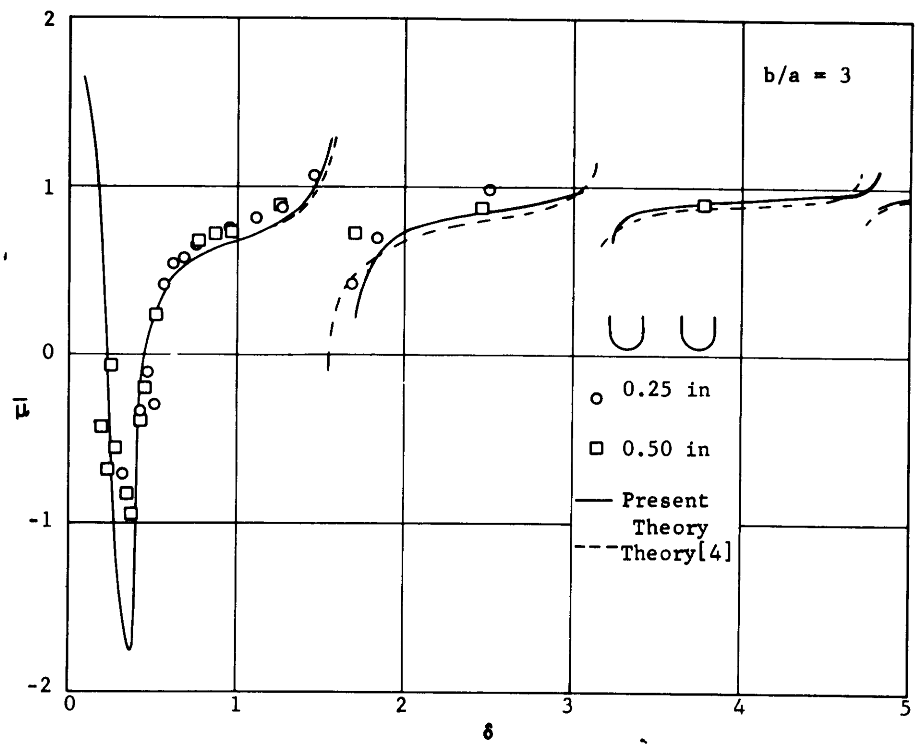

Figure 9 - Added Mass Coefficient versus Frequency Number for Twin Semicircular Cylinders for b/a=3

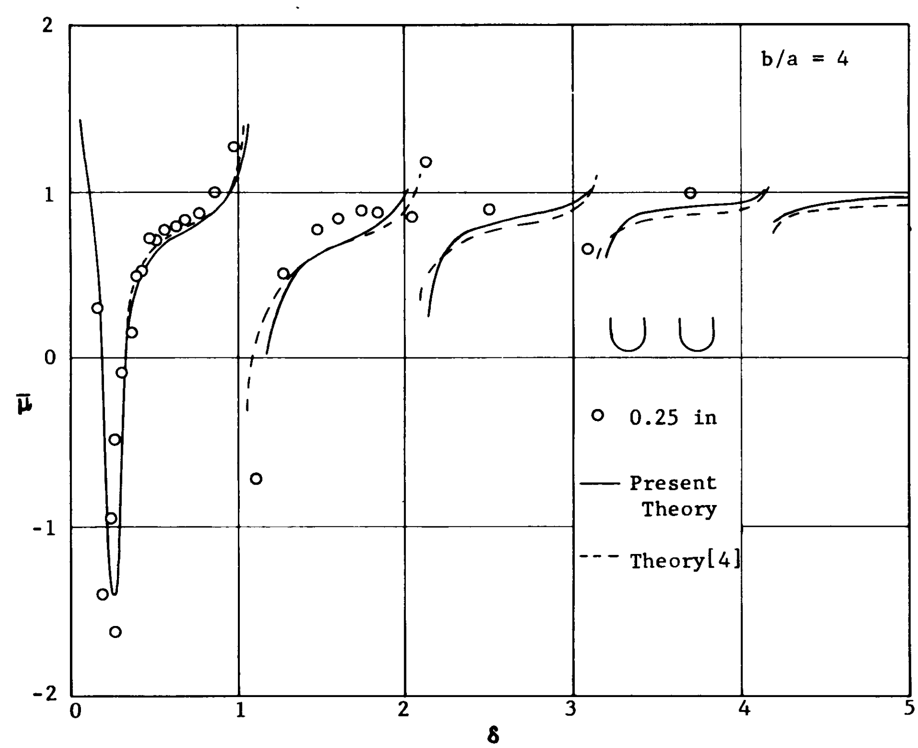

Figure 10 - Added Mass Coefficient versus Frequency Number for Twin Semicircular Cylinders for b/a=4

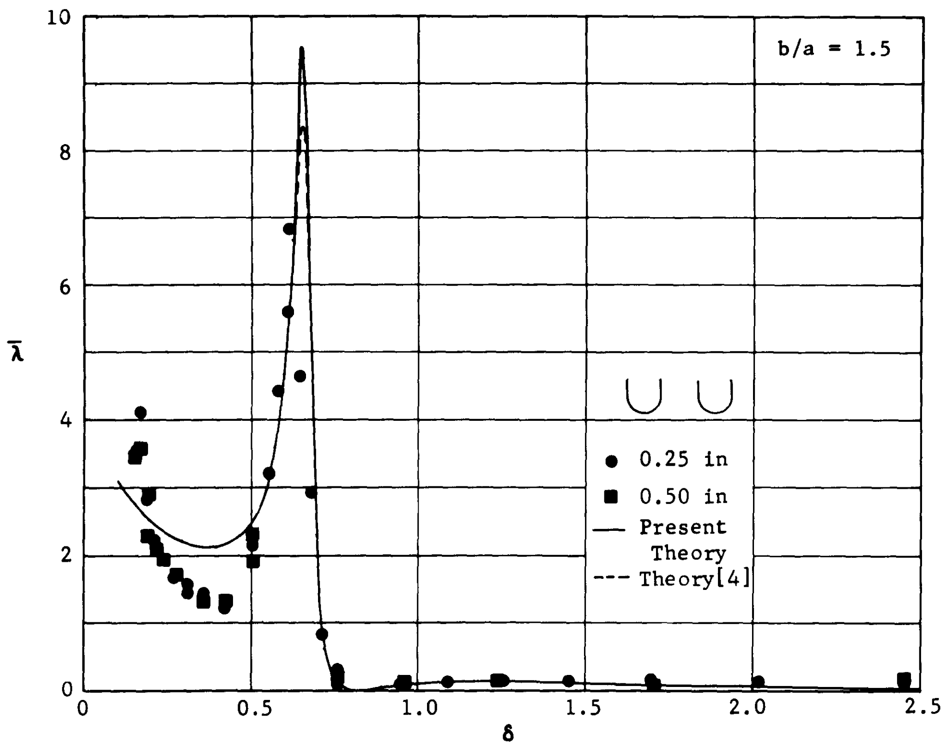

Figure 11 - Damping Coefficient versus Frequency Number for Twin Semicircular Cylinders for b/a=1.5

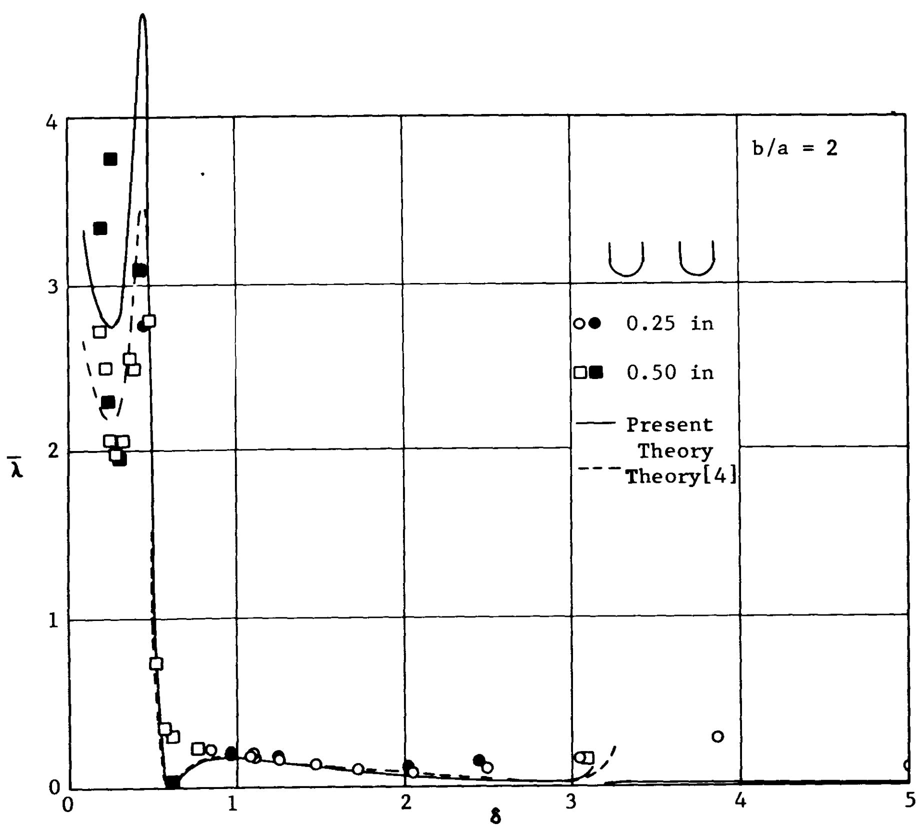

Figure 12 - Damping Coefficient versus Frequency Number for Twin Semicircular Cylinders for b/a=2

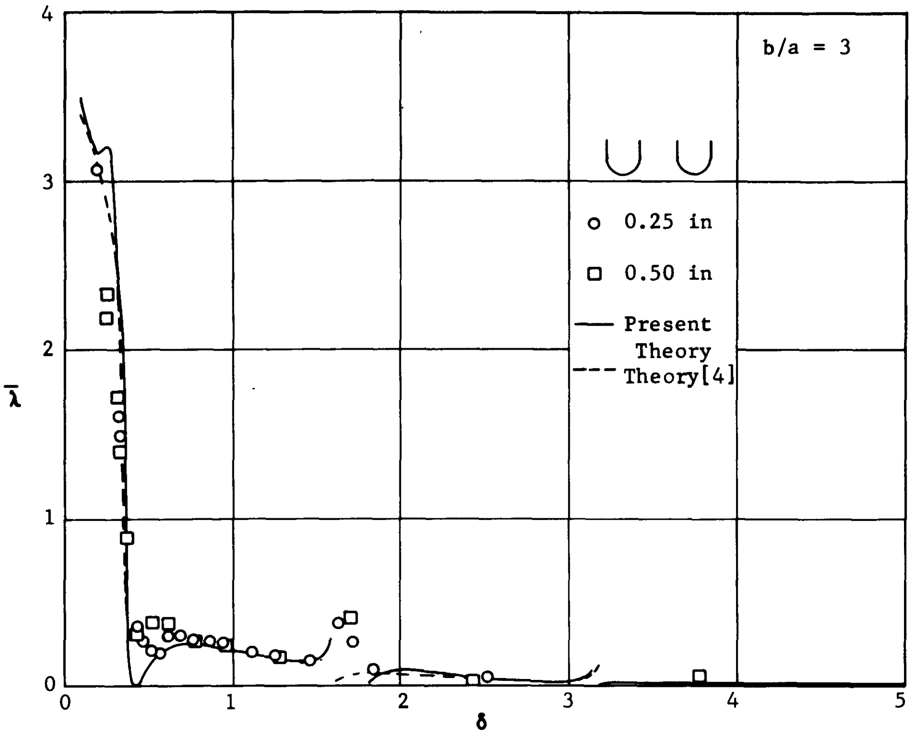

Figure 13 - Damping Coefficient versus Frequency Number for Twin Semicircular Cylinders for b/a=3

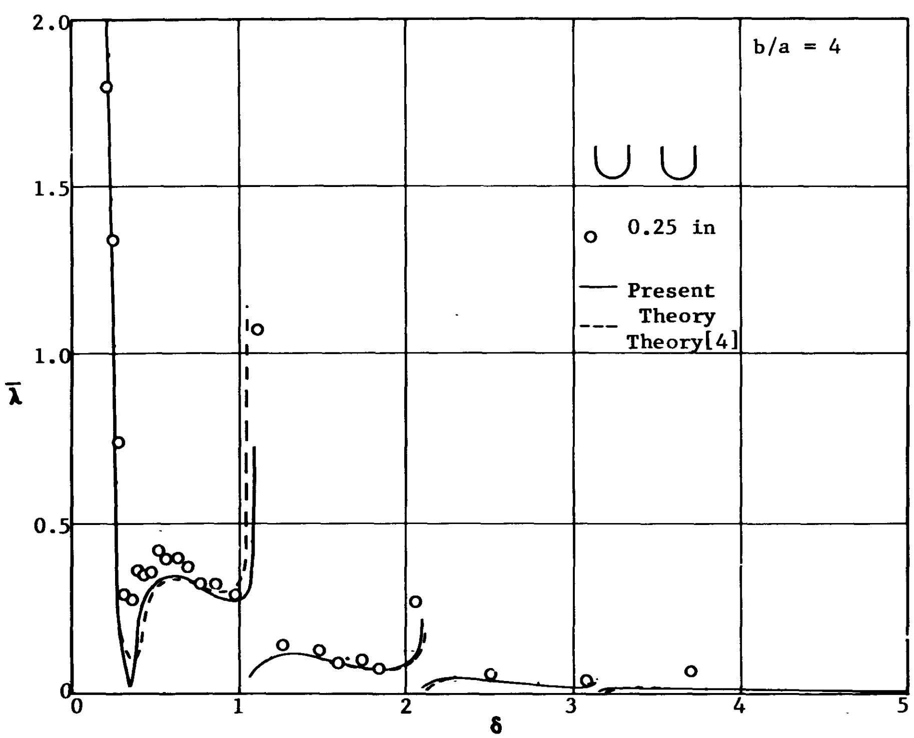

Figure 14 - Damping Coefficient versus Frequency Number for Twin Semicircular Cylinders for b/a=4

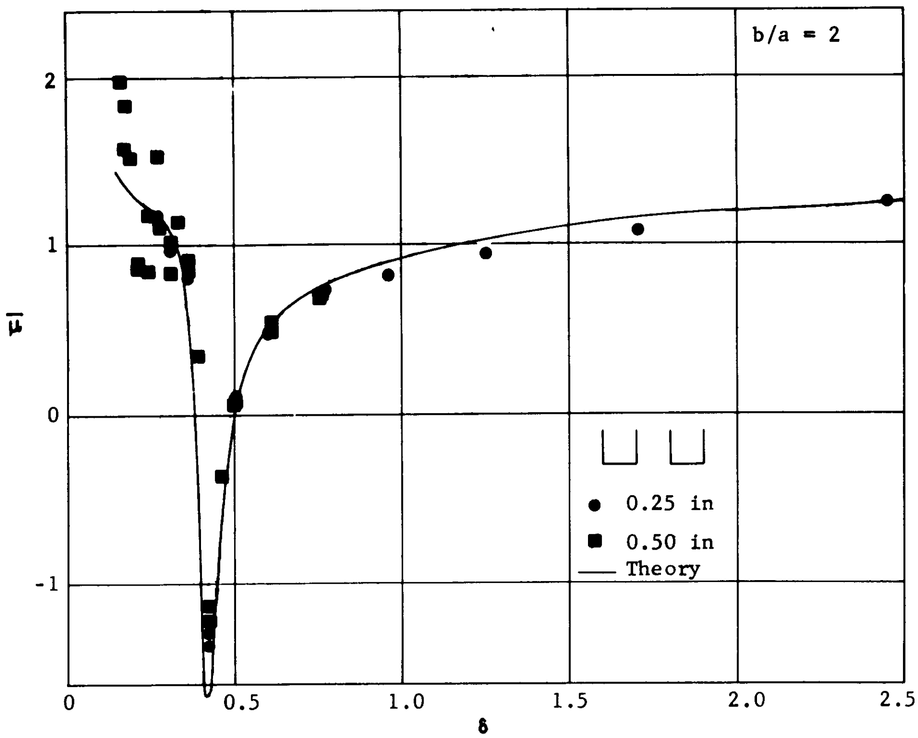

Figure 15 - Added Mass Coefficient versus Frequency Number for Twin Rectangles for b/a=2

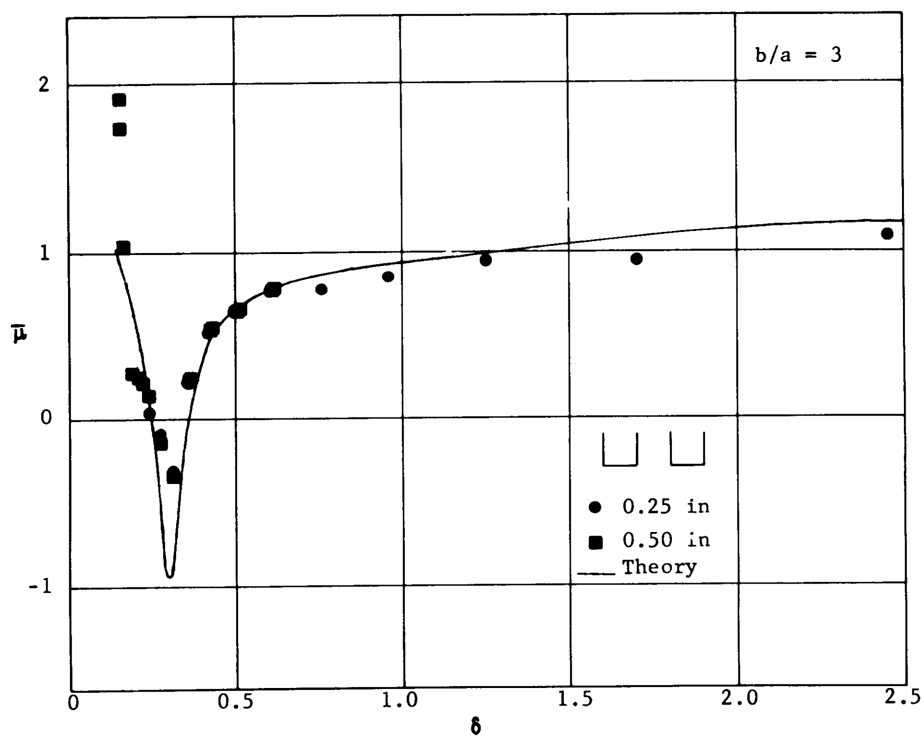

Figure 16 - Added Mass Coefficient versus Frequency Number for Twin Rectangles for b/a=3

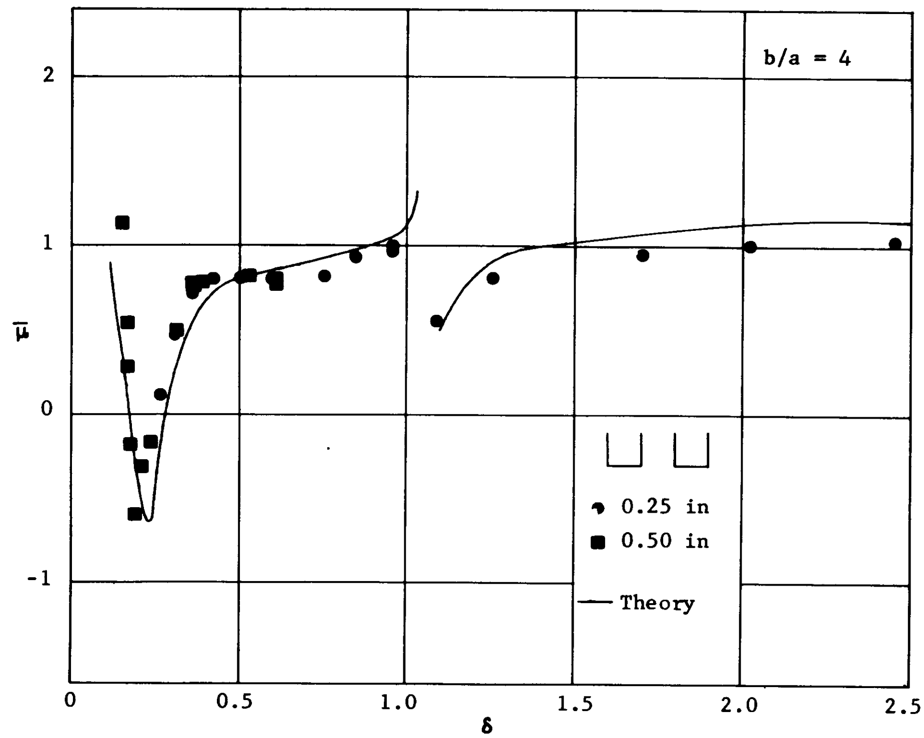

Figure 17 - Added Mass Coefficient versus Frequency Number for Twin Rectangles for b/a=4

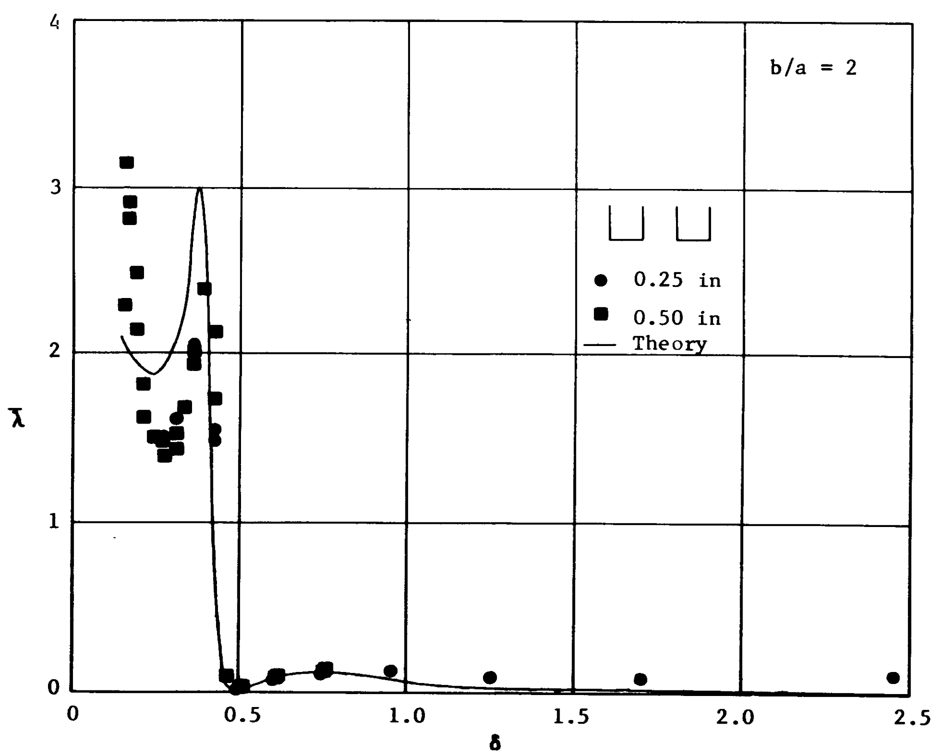

Figure 18 - Damping Coefficient versus Frequency Number for Twin Rectangles for b/a=2

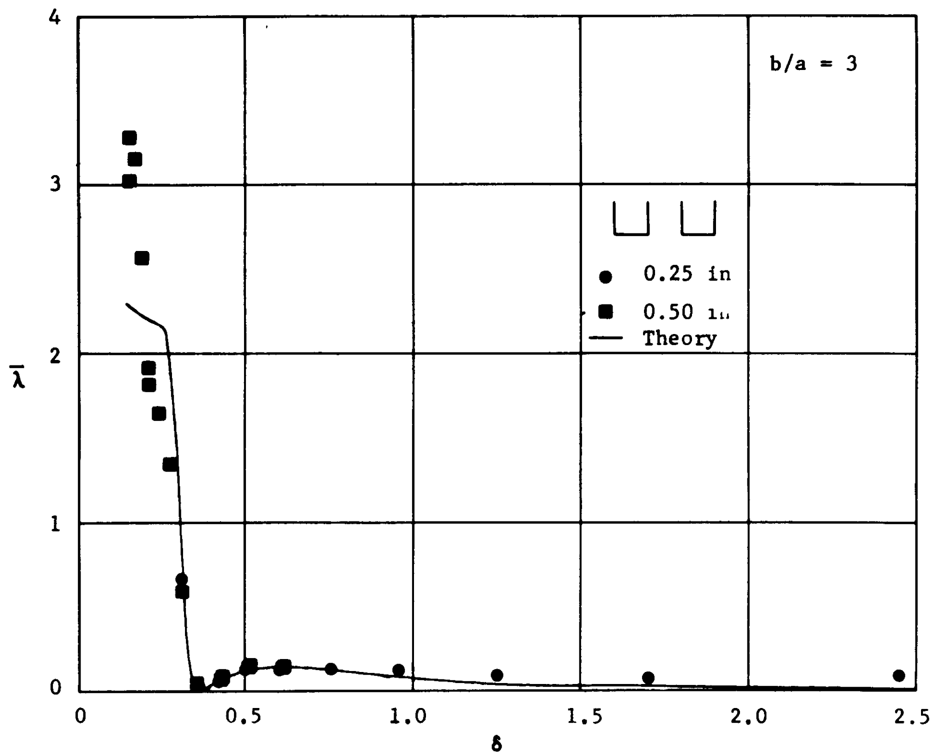

Figure 19 - Damping Coefficient versus Frequency Number for Twin Rectangles for b/a=3

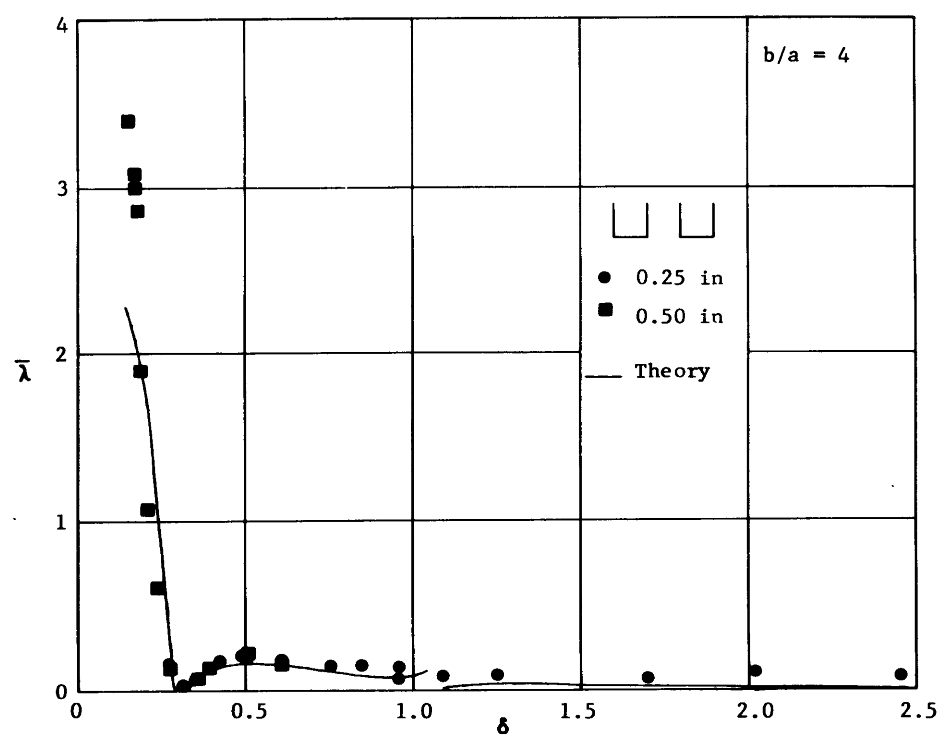

Figure 20 - Damping Coefficient versus Frequency Number for Twin Rectangles for b/a=4

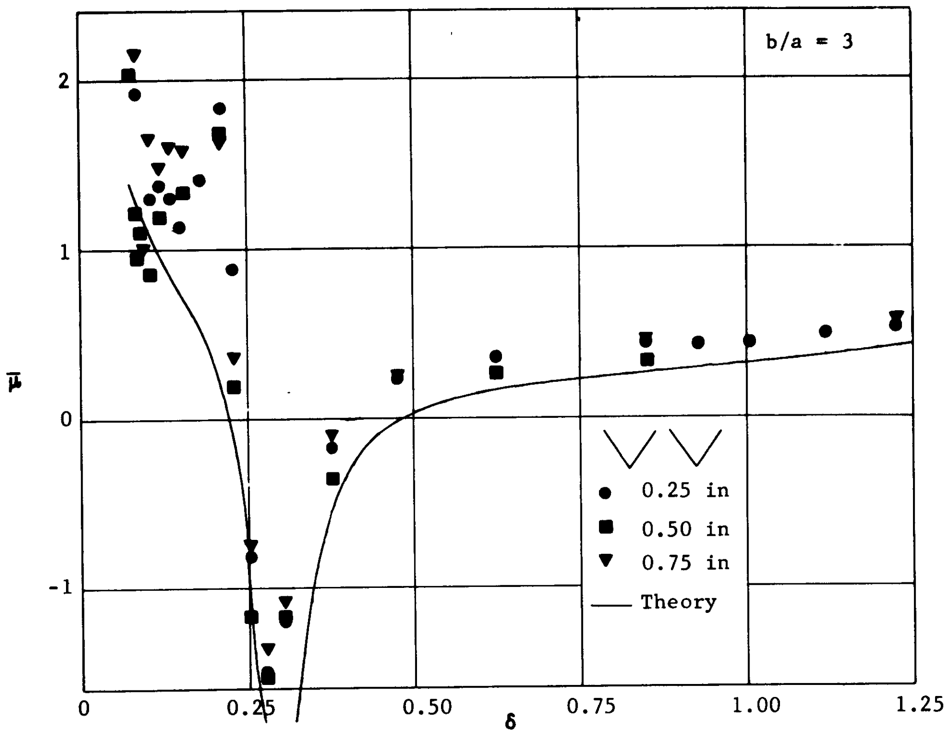

Figure 21 - Added Mass Coefficient versus Frequency Number for Twin Isosceles Triangles for b/a=3

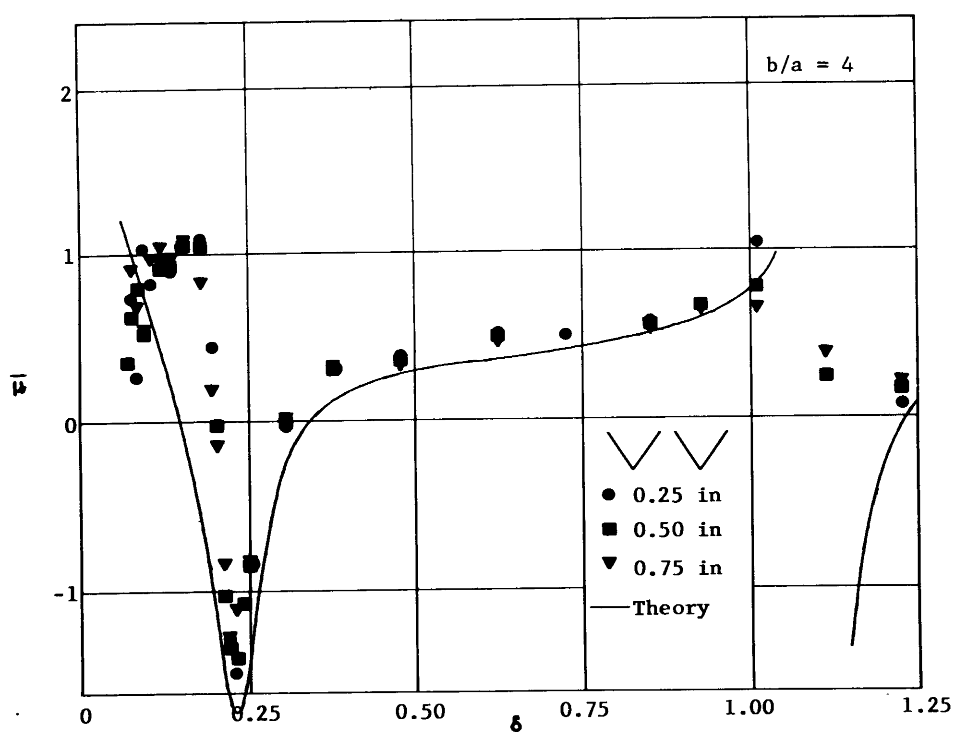

Figure 22 - Added Mass Coefficient versus Frequency Number for Twin Isosceles Triangles for b/a=4

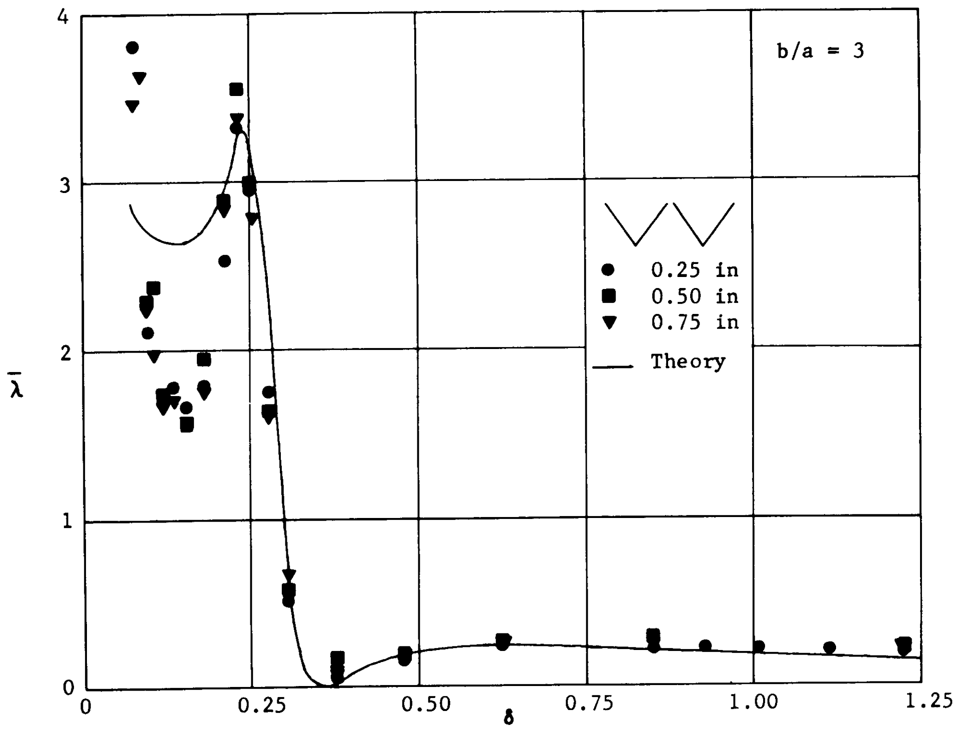

Figure 23 - Damping Coefficient versus Frequency Number for Twin Isosceles Triangles for b/a=3

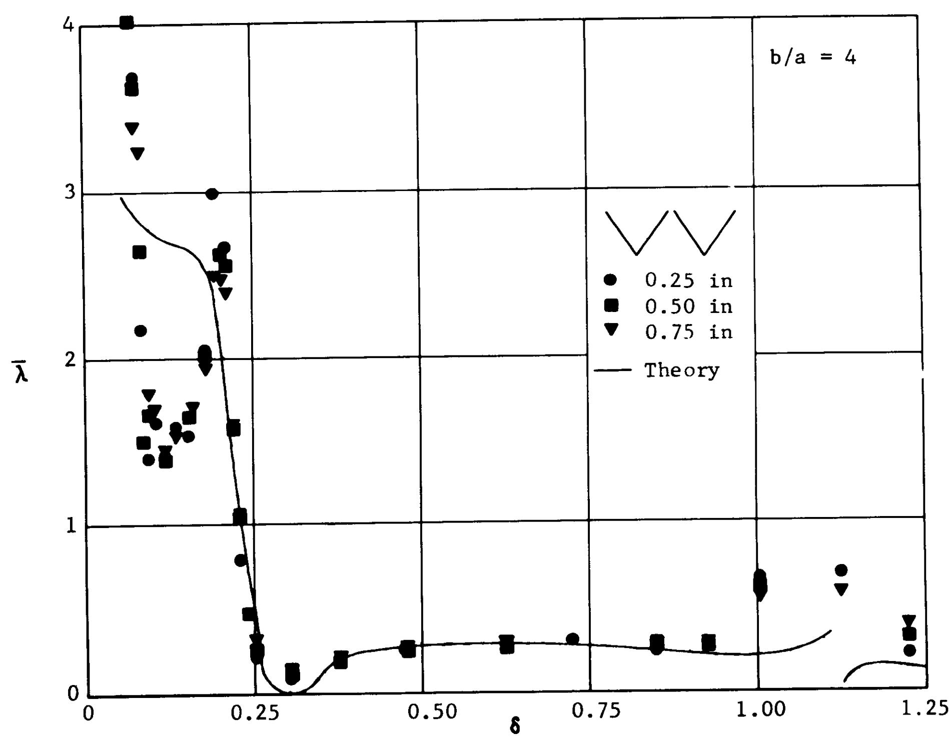

Figure 24 - Damping Coefficient versus Frequency Number for Twin Isosceles Triangles for b/a=4

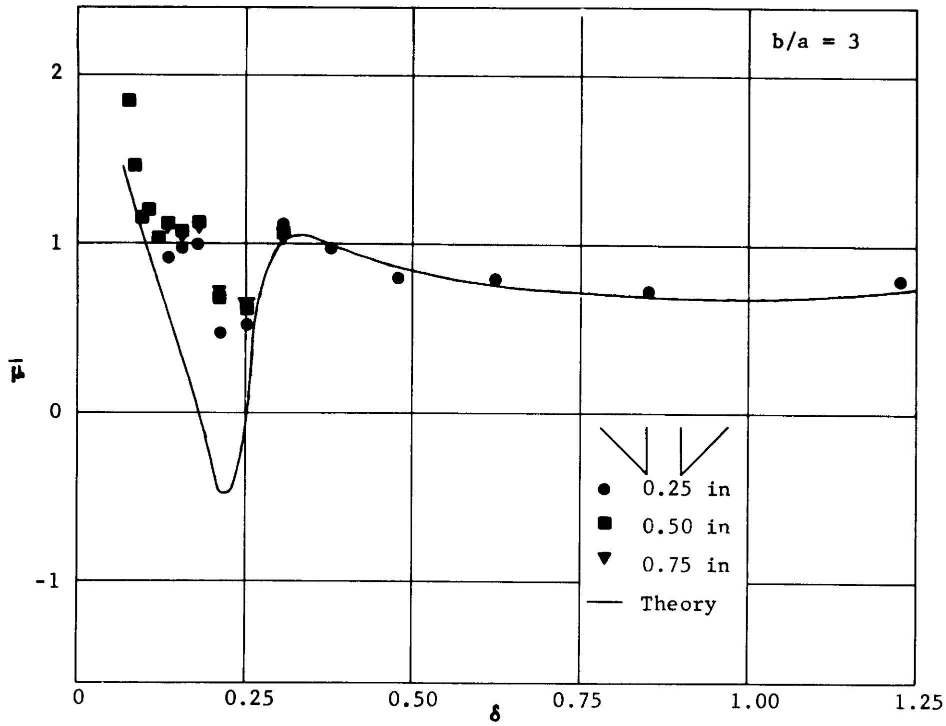

Figure 25 - Added Mass Coefficient versus Frequency Number for Twin Right Triangles for b/a=3

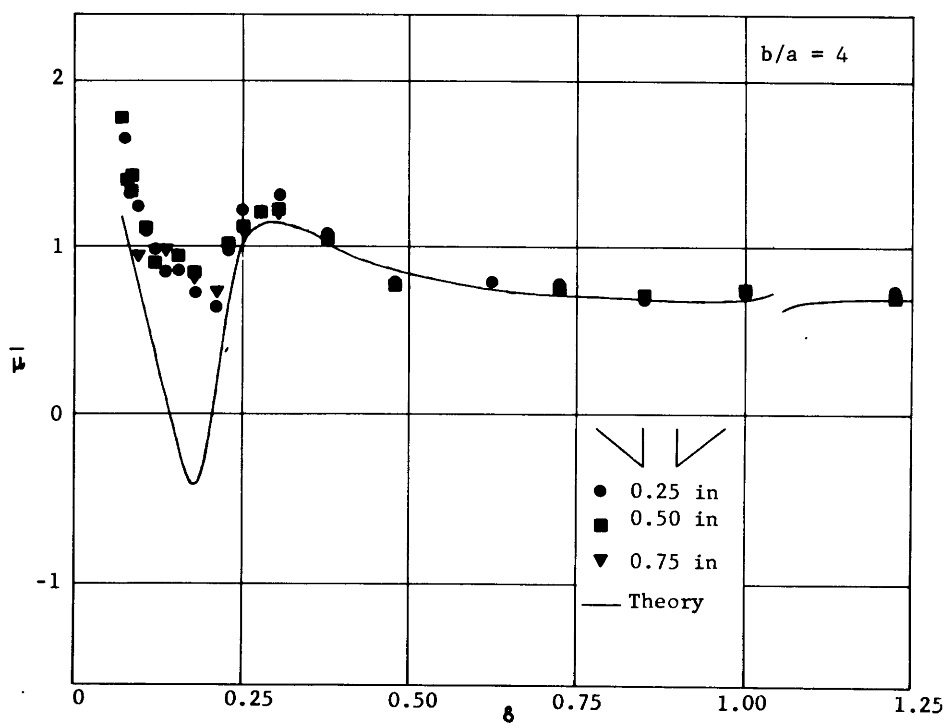

Figure 26 - Added Mass Coefficient versus Frequency Number for Twin Right Triangles for b/a=4

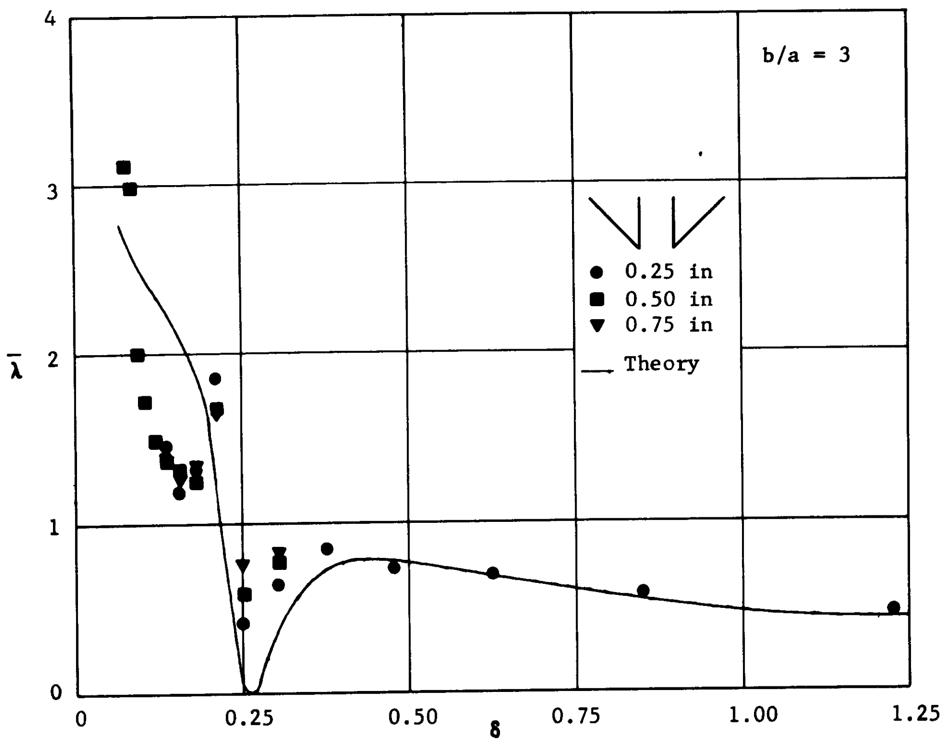

Figure 27 - Damping Coefficient versus Frequency Number for Twin Right Triangles for b/a=3

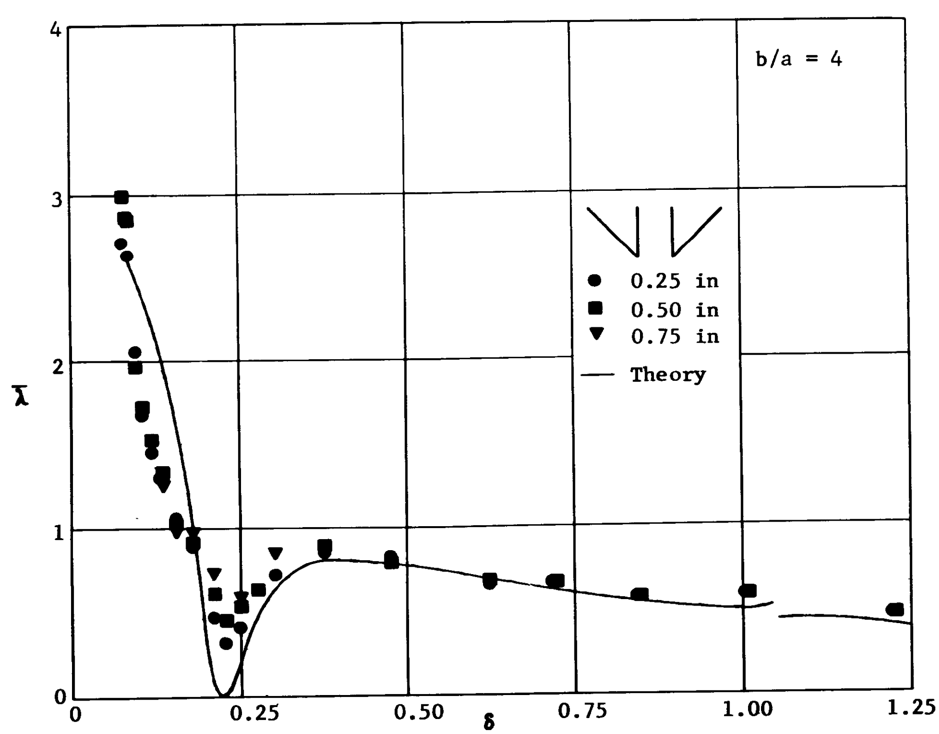

Figure 28 - Damping Coefficient versus Frequency Number for Twin Right Triangles for b/a=4

APPENDIX A
EVALUATION OF MATRIX ELEMENTS

The evaluation of the influence coefficients given by Equations (21) and (22) are

$$I_{ij} = (\underline{n}\cdot\nabla) \int_{c_j} G_{Rc}\,(p;s)\,ds\Big|_{p=p_i} \tag{33}$$

$$J_{ij} = (\underline{n}\cdot\nabla) \int_{c_j} G_{Rs}\,(p;s)\,ds\Big|_{p=p_i} \tag{34}$$

From Equation (15) we find that

$$G_{Rc}\,(z;\zeta) = \frac{1}{2\pi}\,\mathrm{Re}_i\left\{\log\frac{(z-\zeta)(z+\bar{\zeta})}{(z-\bar{\zeta})(z+\zeta)} + 2\int_0^\infty \frac{e^{-ik\,(z-\bar{\zeta})} + e^{-ik\,(z+\zeta)}}{K-k}\,dk\right\} \tag{35}$$

$$G_{Rs}\,(z;\zeta) = -\mathrm{Re}_i\left\{e^{-iK(z-\bar{\zeta})} + e^{-iK(z+\zeta)}\right\} \tag{36}$$

If we let a_i denote the tangent angle of the ith segment c_i of the cylinder contour, i.e.,

$$a_i = \tan^{-1}\frac{(y_{i+1} - y_i)}{(x_{i+1} - x_i)}$$

we have

$$\underline{n}\Big|_{c_i} = (\sin a_i, -\cos a_i)$$

Thus, for any analytic function f(z)

$$\mathrm{Re}_i\left\{(n\cdot\nabla)\,f(z)\Big|_{z=z_i}\right\} = \mathrm{Re}_i\left[\left\{\sin a\,\frac{\partial}{\partial x} - \cos a\,\frac{\partial}{\partial y}\right\} f(z)\Big|_{\substack{z=z_i\\ a=a_i}}\right]$$

$$= \mathrm{Re}_i\left(-ie^{ia_i}\,\frac{d}{dz}f(z)\Big|_{z=z_i}\right) \tag{37}$$

We can also show that for $\zeta \epsilon\, c_o$

$$d\zeta = d\xi + id\eta = e^{ia}ds \tag{38}$$

where a is the tangent angle at the point ζ, and

$$d\bar{\zeta} = e^{-ia} ds \tag{39}$$

We substitute Equation (35) into (33) to derive

$$I_{ij} = \frac{1}{2\pi} Re_i \Big\{ (\underline{n}\cdot\nabla) \int_{C_j} \log(z-\zeta)\, ds \Big|_{z=z_i}$$

$$- (\underline{n}\cdot\nabla) \int_{C_j} \log(z-\bar{\zeta})\, ds \Big|_{z=z_i}$$

$$+ 2(\underline{n}\cdot\nabla) \int_{C_j} ds \int_0^\infty \frac{e^{-ik(z+\zeta)}}{K-k}\, dk \Big|_{z=z_i} \Big\} \tag{40}$$

where $z_i = x_i + iy_i$ is assumed to be located at the midpoint of the ith segment.

Utilizing Equations (35) through (37), we can show that

$$L_1 \equiv Re_i \Big\{ (\underline{n}\cdot\nabla) \int_{C_j} \log(z-\zeta)\, ds \Big|_{z=z_i} \Big\}$$

$$= Re_i \Big\{ - ie^{ia_i} \frac{d}{dz} \int_{\zeta_j}^{\zeta_{j+1}} \log(z-\zeta')\, e^{-ia_j} d\zeta' \Big|_{z=z_i} \Big\}$$

$$= Re_i \Big[- ie^{i(a_i-a_j)} \frac{d}{dz} \Big\{ (z-\zeta') - (z-\zeta')\log(z-\zeta') \Big|_{\zeta_j}^{\zeta_{j+1}} \Big\} \Big|_{z=z_i} \Big]$$

$$= Re_i \Big\{ ie^{i(a_i-a_j)} \log \frac{z_i-\zeta_{j+1}}{z_i-\zeta_j} \Big\}$$

$$= \tfrac{1}{2} \sin(a_i-a_j) \log \frac{(x_i-\xi_j)^2+(y_i-\eta_j)^2}{(x_i-\xi_{j+1})^2+(y_i-\eta_{j+1})^2}$$

$$+ \cos(a_i-a_j) \Big\{ \tan^{-1} \frac{y_i-\eta_j}{x_i-\xi_j} - \tan^{-1} \frac{y_i-\eta_{j+1}}{x_i-\xi_{j+1}} \Big\} , \tag{41}$$

$$L_2 \equiv Re_i \Big\{ (\underline{n}\cdot\nabla) \int_{C_j} \log(z-\bar{\zeta})\, ds \Big|_{z=z_i} \Big\}$$

$$= Re_i \Big\{ - ie^{i(a_i+a_j)} \frac{d}{dz} \int_{\bar{\zeta}_j}^{\bar{\zeta}_{j+1}} \log(z-\zeta')\, d\zeta' \Big|_{z=z_i} \Big\}$$

$$= \tfrac{1}{2} \sin(a_i + a_j) \log \frac{(x_i - \xi_j)^2 + (y_i - \eta_j)^2}{(x_i - \xi_{j+1})^2 + (y_i + \eta_{j+1})^2}$$

$$+ \cos(a_i + a_j) \left\{ \tan^{-1} \frac{y_i + \eta_j}{x_i - \xi_j} - \tan^{-1} \frac{y_i + \eta_{j+1}}{x_i - \xi_{j+1}} \right\}, \tag{42}$$

$$L_3 \equiv \mathrm{Re}_i \left\{ (\underline{n} \cdot \nabla) \int_{c_j} \log(z + \bar{\zeta})\, ds \bigg|_{z = z_i} \right\}$$

$$= -\tfrac{1}{2} \sin(a_i + a_j) \log \frac{(x_i + \xi_j)^2 + (y_i - \eta_j)^2}{(x_i + \xi_{j+1})^2 + (y_i - \eta_{j+1})^2}$$

$$- \cos(a_i + a_j) \left\{ \tan^{-1} \frac{y_i - \eta_j}{x_i + \xi_j} - \tan^{-1} \frac{y_i - \eta_{j+1}}{x_i - \xi_{j+1}} \right\}, \tag{43}$$

$$L_4 \equiv \mathrm{Re}_i \left\{ (\underline{n} \cdot \nabla) \int_{c_j} \log(z + \zeta)\, ds \bigg|_{z = z_i} \right\}$$

$$= -\tfrac{1}{2} \sin(a_i - a_j) \log \frac{(x_i + \xi_j)^2 + (y_i + \eta_j)^2}{(x_i + \xi_{j+1})^2 + (y_i + \eta_{j+1})^2}$$

$$- \cos(a_i - a_j) \left\{ \tan^{-1} \frac{y_i + \eta_j}{x_i + \xi_j} - \tan^{-1} \frac{y_i + \eta_{j+1}}{x_i + \xi_{j+1}} \right\}, \tag{44}$$

$$L_5 \equiv \mathrm{Re}_i \left\{ (\underline{n} \cdot \nabla) \int_{c_j} ds \int_0^\infty \frac{e^{-ik(z - \bar{\zeta})}}{K - k}\, dk \bigg|_{z = z_i} \right\}$$

$$= \mathrm{Re}_i \left\{ -ie^{i(a_i + a_j)} \frac{d}{dz} \int_{\bar{\zeta}_j}^{\bar{\zeta}_{j+1}} d\zeta' \int_0^\infty \frac{e^{-ik(z - \zeta')}}{K - k}\, dk \bigg|_{z = z_i} \right\}$$

$$= \mathrm{Re}_i \left\{ -ie^{i(a_i + a_j)} \left(-\frac{d}{d\bar{\zeta}}\right) \int_{\bar{\zeta}_j}^{\bar{\zeta}_{j+1}} d\zeta' \int_0^\infty \frac{e^{-ik(z - \zeta')}}{K - k}\, dk \bigg|_{z = z_i} \right\}$$

$$= \mathrm{Re}_i \left\{ -ie^{i(a_i + a_j)} \int_0^\infty \frac{e^{-ik(z - \bar{\zeta}_j)} - e^{-ik(z_i - \bar{\zeta}_{j+1})}}{K - k}\, dk \right\}$$

$$= \sin(a_i + a_j) \int_0^\infty \frac{dk}{K - k} \left\{ e^{k(y_i + \eta_j)} \cos k(x_i - \xi_j) - e^{k(y_i + \eta_{j+1})} \cos k(x_i + \xi_{j+1}) \right\}$$

$$-\cos(a_i+a_j)\int_0^{\infty}\frac{dk}{K-k}\left\{e^{k(y_i+\eta_j)}\sin k(x_i-\xi_j)-e^{k(y_i+\eta_{j+1})}\sin k(x_i-\xi_{j+1})\right\}, \quad (45)$$

$$L_6 \equiv \mathrm{Re}_i\left\{(\underline{n}\cdot\nabla)\int_{C_j}ds\int_0^{\infty}\frac{e^{-ik(z+\bar{\zeta})}}{K-k}dk\bigg|_{z=z_i}\right\}$$

$$= -\sin(a_i-a_j)\int_0^{\infty}\frac{dk}{K-k}\left\{e^{k(y_i+\eta_j)}\cos k(x_i+\xi_j)-e^{k(y_i+\eta_{j+1})}\cos k(x_i+\xi_{j+1})\right\}$$

$$+\cos(a_i-a_j)\int_0^{\infty}\frac{dk}{K-k}\left\{e^{k(y_i+\eta_j)}\sin k(x_i+\xi_j)-e^{k(y_i+\eta_{j+1})}\sin k(x_i+\xi_{j+1})\right\} \quad (46)$$

Substituting Equation (36) into Equation (34), we obtain the following integrals:

$$L_7 \equiv \mathrm{Re}_i\left\{(\underline{n}\cdot\nabla)\int_{C_j}e^{-iK(z-\bar{\zeta})}\,ds\bigg|_{z=z_i}\right\}$$

$$= \mathrm{Re}_i\left\{-ie^{i(a_i+a_j)}\left(-\frac{d}{d\bar{\zeta}}\right)\int_{\bar{\zeta}_j}^{\bar{\zeta}_{j+1}}e^{-iK(z-\zeta')}\,d\zeta'\right\}$$

$$= \sin(a_i+a_j)\left\{e^{K(y_i+\eta_j)}\cos K(x_i-\xi_j)-e^{K(y_i+\eta_{j+1})}\cos K(x_i-\xi_{j+1})\right\}$$

$$-\cos(a_i+a_j)\left\{e^{K(y_i+\eta_j)}\sin K(x_i-\xi_j)-e^{K(y_i+\eta_{j+1})}\sin K(x_i-\xi_{j+1})\right\} \quad (47)$$

$$L_8 \equiv \mathrm{Re}_i\left\{(\underline{n}\cdot\nabla)\int_{C_j}e^{-iK(z+\bar{\zeta})}ds\bigg|_{z=z_i}\right\}$$

$$= -\sin(a_i-a_j)\left\{e^{K(y_i+\eta_j)}\cos K(x_i+\xi_j)-e^{K(y_i+\eta_{j+1})}\cos K(x_i+\xi_{j+1})\right\}$$

$$+\cos(a_i-a_j)\left\{e^{K(y_i+\eta_j)}\sin K(x_i+\xi_j)-e^{K(y_i+\eta_{j+1})}\sin K(x_i+\xi_{j+1})\right\} \quad (48)$$

Combining the previous results, we can finally show that

$$I_{ij} = \frac{1}{2\pi}(L_1-L_2+L_3-L_4+2L_5+2L_6) \quad (49)$$

and

$$J_{ij} = -L_7 - L_8 \tag{50}$$

The evaluation of the principal value integrals in Equations (45) and (46), which can be converted to the exponential integral, are shown in Appendix C.

APPENDIX B
EVALUATION OF POTENTIAL INTEGRALS

To obtain the hydrodynamic coefficients, we must know the values of the velocity potentials on the cylinder surface. The expressions for the velocity potentials are given by Equations (24) and (25) which contain the integrals,

$$I_1 \equiv \int_{c_j} G_{Rc}\,(p_o\,;s)\,ds$$

and

$$I_2 \equiv \int_{c_j} G_{Rs}\,(p_o\,;s)\,ds$$

where p_o is a point on the cylinder contour and c_j is a line segment of the cylinder contour.

We shall use the complex expression given by Equation (15) to evaluate the integrals I_1 and I_2. Thus, for the point $z_i = x_i + iy_i$ which is located at the midpoint of the line segment c_i, we have

$$I_1 = \frac{1}{2\pi}\,\mathrm{Re}_i\left[\int_{c_j} ds\left\{\log(z_i-\zeta) - \log(z_i-\bar{\zeta}) + \log(z_i+\bar{\zeta}) - \log(z_i+\zeta) + 2\!\!\!\!\!\!\!\int_0^\infty \frac{e^{-ik(z_i-\bar{\zeta})}}{K-k}\,dk + 2\!\!\!\!\!\!\!\int_0^\infty \frac{e^{-ik(z_i+\zeta)}}{K-k}\,dk\right\}\right] \tag{51}$$

$$I_2 = -\mathrm{Re}_i\left\{\int_{c_j} e^{-iK(z_i-\bar{\zeta})}ds + \int_{c_j} e^{-iK(z_i+\zeta)}ds\right\} \tag{52}$$

We can easily show by using the relations given by Equations (38) and (39) in Appendix A that

$$K_1 \equiv \mathrm{Re}_i \int_{c_j} \log(z_i-\zeta)\,ds$$

$$= \mathrm{Re}_i\left[e^{-i\alpha_j}\left\{(z_i-\zeta) - (z_i-\zeta)\log(z-\zeta)\Big|_{\zeta_j}^{\zeta_{j+1}}\right\}\right]$$

$$
\begin{aligned}
= \cos a_j \Big\{ & \xi_j - \xi_{j+1} + (x_i - \xi_j) \log|z_i - \zeta_j| \\
& - (x_i - \xi_{j+1}) \log|z_i - \zeta_{j+1}| - (y_i - \eta_j) \arg(z_i - \zeta_{j+1}) \\
& + (y_i - \eta_{j+1}) \arg(z_i - \zeta_{j+1}) \Big\} \\
& + \sin a_j \Big\{ \eta_j - \eta_{j+1} + (y_i - \eta_j) \log|z_i - \zeta_j| \\
& - (y_i - \eta_{j+1}) \log|z_i - \zeta_{j+1}| + (x_i - \xi_j) \arg(z_i - \zeta_j) \\
& - (x_i - \xi_{j+1}) \arg(z_i - \zeta_{j+1}) \Big\}
\end{aligned} \tag{53}
$$

where

$$
|z - \zeta| = \Big\{ (x - \xi)^2 + (y - \eta)^2 \Big\}^{1/2}
$$

$$
\arg(z - \zeta) = \tan^{-1} \frac{y - \eta}{x - \xi}
$$

If we define

$$
I(x_i, y_i; \xi_j^{j+1}, \eta_j^{j+1}; a_j) = \mathrm{Re}_i \int_{C_j} \log(z_i - \zeta)\, ds
$$

the remaining integrals involving logarithmic functions in Equation (51) can be given by

$$
K_2 \equiv \mathrm{Re}_i \int_{C_j} \log(z_i - \bar{\zeta})\, ds = I(x_i, y_i; \xi_j^{j+1}, -\eta_j^{j+1}; -a_j) \tag{54}
$$

$$
K_3 \equiv \mathrm{Re}_i \int_{C_j} \log(z_i + \bar{\zeta})\, ds = -I(x_i, y_i; -\xi_j^{j+1}, \eta_j^{j+1}; -a_j) \tag{55}
$$

$$
K_4 \equiv \mathrm{Re}_i \int_{C_j} \log(z_i + \zeta)\, ds = -I(x_i, y_i; -\xi_j^{j+1}, -\eta_j^{j+1}; -a_j) \tag{56}
$$

If we again define

$$
K_5 \equiv \mathrm{Re}_i \Big\{ \int_{C_j} ds \;⨍_0^{\infty} \frac{e^{-ik(z_i - \bar{\zeta})}}{K - k}\, dk \Big\}
$$

we can show that

$$K_5 = \mathrm{Re}_i \left\{ e^{i\alpha_j} \int_0^\infty \frac{dk}{K-k} \int_{\bar{\zeta}_j}^{\bar{\zeta}_{j+1}} e^{-ik(z_i - \zeta')} d\zeta' \right.$$

$$= \mathrm{Re}_i \left\{ -ie^{i\alpha_j} \int_0^\infty \frac{e^{-ikz_i}}{K-k} \frac{e^{ik\bar{\zeta}_{j+1}} - e^{ik\bar{\zeta}_j}}{k} dk \right\}$$

By use of partial fractions

$$\frac{1}{(K-k)k} = \frac{1}{K}\left(\frac{1}{K-k} + \frac{1}{k}\right)$$

we get

$$K_5 = \mathrm{Re}_i \left[-\frac{ie^{i\alpha_j}}{K} \left\{ \int_0^\infty \frac{e^{-ik(z_i - \bar{\zeta}_{j+1})} - e^{-ik(z_i - \bar{\zeta}_j)}}{k} dk \right.\right.$$

$$\left.\left. + \int_0^\infty \frac{e^{-ik(z_i - \bar{\zeta}_{j+1})} - e^{-ik(z_i - \bar{\zeta}_j)}}{K-k} dk \right\} \right] \quad (57)$$

The first integral in Equation (57) can be regarded as a function of z and can be written as

$$F(z) = \int_0^\infty \frac{e^{-ik(z - \bar{\zeta}_{j+1})} - e^{-ik(z - \bar{\zeta}_j)}}{k} dk$$

Then, we have

$$F'(z) = -i \int_0^\infty \left\{ e^{-ik(z - \bar{\zeta}_{j+1})} - e^{-ik(z - \bar{\zeta}_j)} \right\} dk$$

$$= \frac{1}{z - \bar{\zeta}_j} - \frac{1}{z - \bar{\zeta}_{j+1}}$$

from which

$$F(z) = \log \frac{z - \bar{\zeta}_j}{z - \bar{\zeta}_{j+1}}$$

where we let the arbitrary integral constant be zero to satisfy the deepwater condition as given by Equation (9).

Substituting the previous results into Equation (57), we have

$$K_5 = \mathrm{Re}_i \left[-\frac{ie^{i\alpha_j}}{K} \left\{ \log \frac{z_i - \bar{\zeta}_j}{z_i - \bar{\zeta}_{j+1}} + \int_0^\infty \frac{e^{-ik(z_i - \bar{\zeta}_{j+1})} - e^{-ik(z_i - \bar{\zeta}_j)}}{K-k} dk \right\} \right]$$

$$= \frac{1}{K} \left[\frac{1}{2} \sin \alpha_j \left\{ \log \frac{(x_i - \xi_j)^2 + (y_i + \eta_j)^2}{(x_i - \xi_{j+1})^2 + (y_i + \eta_{j+1})^2} \right. \right.$$

$$+ \int_0^\infty \frac{dk}{K-k} \left\{ e^{k(y_i + \eta_{j+1})} \cos k(x_i - \xi_{j+1}) \right.$$

$$\left. \left. - e^{k(y_i + \eta_j)} \cos k(x_i - \xi_j) \right\} \right\}$$

$$+ \cos \alpha_j \left\{ \tan^{-1} \frac{y_i + \eta_j}{x_i - \xi_j} - \tan^{-1} \frac{y_i - \eta_{j+1}}{x_i - \xi_{j+1}} \right.$$

$$\left. \left. + \int_0^\infty \frac{dk}{K-k} \left\{ e^{k(y_i + \eta_j)} \sin k(x_i - \xi_j) - e^{k(y_i + \eta_{j+1})} \sin k(x_i - \xi_{j+1}) \right\} \right\} \right] \tag{58}$$

If we let

$$K_5 = L(x_i, y_i; \xi_j^{j+1}, \eta_j^{j+1}; \alpha_j),$$

we can show that

$$K_6 \equiv \mathrm{Re}_i \left\{ \int_{C_j} ds \int_0^\infty \frac{d^{-ik(z_i + \zeta)}}{K-k} dk \right\} = L(x_i, y_i; -\xi_j^{j+1}, \eta_j^{j+1}; -\alpha_j) \tag{59}$$

The integrals in Equation (52) can be readily evaluated as

$$K_7 \equiv \mathrm{Re}_i \left\{ \int_{C_j} e^{-iK(z - \bar{\zeta})} ds \right\} = \mathrm{Re}_i \left\{ \int_{\bar{\zeta}_j}^{\bar{\zeta}_{j+1}} e^{-i} \left\{ K(z - \zeta') - \alpha_j \right\} d\zeta' \right\}$$

$$= \frac{1}{K} \left[e^{K(y_i + \eta_j)} \sin \left\{ K(x_i - \xi_j) - \alpha_j \right\} - e^{K(y_i + \eta_{j+1})} \sin \left\{ K(x_i + \xi_{j+1}) - \alpha_j \right\} \right] \tag{60}$$

$$K_8 \equiv \mathrm{Re}_i\left\{ \int_{C_j} e^{-iK(z+\zeta)} ds \right\} = \mathrm{Re}_i\left\{ \int_{\zeta_j}^{\zeta_{j+1}} e^{-i\{K(z+\zeta')+\alpha_j\}} d\zeta' \right\}$$

$$= \frac{1}{K}\left[e^{K(y_i+\eta_{j+1})} \sin\left\{ K(x_i+\xi_{j+1}) + \alpha_j \right\} - e^{K(y+\eta_j)} \sin\left\{ K(x_i+\xi_j) + \alpha_j \right\} \right] \tag{61}$$

Combining the results obtained from Equations (53) through (61), we can show that

$$I_1 = \frac{1}{2\pi}(K_1 - K_2 + K_3 - K_4) + \frac{1}{\pi}(K_5 + K_6) \tag{62}$$

$$I_2 = -K_7 - K_8 \tag{63}$$

The principal value integrals in Equations (58) and (59) can be expressed in the form of the exponential integral, which can be easily converted to an infinite series. The details of this procedure are given in Appendix C.

APPENDIX C
EVALUATION OF THE PRINCIPAL VALUE INTEGRALS

In the derivation of Green's function G (z; ζ), which can be interpreted as a wave source near a vertical wall, the principal-value integrals were encountered as shown in Equation (15). These integrals can be reduced to the exponential integral which can be expanded to an infinite series.

We show below how to make this conversion. We have

$$\int_{0}^{\infty} \frac{e^{-ik(z-\bar{\zeta})}}{K-k}\, dk = -\!\!\!\!\!\!\int_{0}^{\infty} \frac{e^{-ik(z-\bar{\zeta})}}{K-k}\, dk + i\pi e^{-iK(z-\bar{\zeta})} \qquad (64)$$

where $\int_0^{\infty}$ (indented path) indicates that the path of the integration is indented above the pole at k=K, and the last term above is the residue value at the pole. Let us first concentrate on the integral on the left-hand side of Equation (64). If we make the transformation

$$w = i(k-K)(z-\bar{\zeta}) \qquad (65)$$

where $k = k_R + ik_I$ and $w = w_R + iw_I$

we can show that

$$w = -k_I(x-\xi)-(k_R-K)(y+\eta) + i\left\{(k_R-K)(x-\xi)-k_I(y+\eta)\right\} \qquad (66)$$

Noting that the path of the integral limits the values of k confined to k_R, $k_I>0$ and that $y+\eta<0$, we apply the transformation of Equation (65) into the integral

$$\int_{0}^{\infty} \frac{e^{-ik(z-\bar{\zeta})}}{K-k}\, dk$$

As shown in Figures 29 and 30, the path of the integral in the k-plane changes to the two different paths, depending on whether $x-\xi>0$ or $x-\xi<0$.

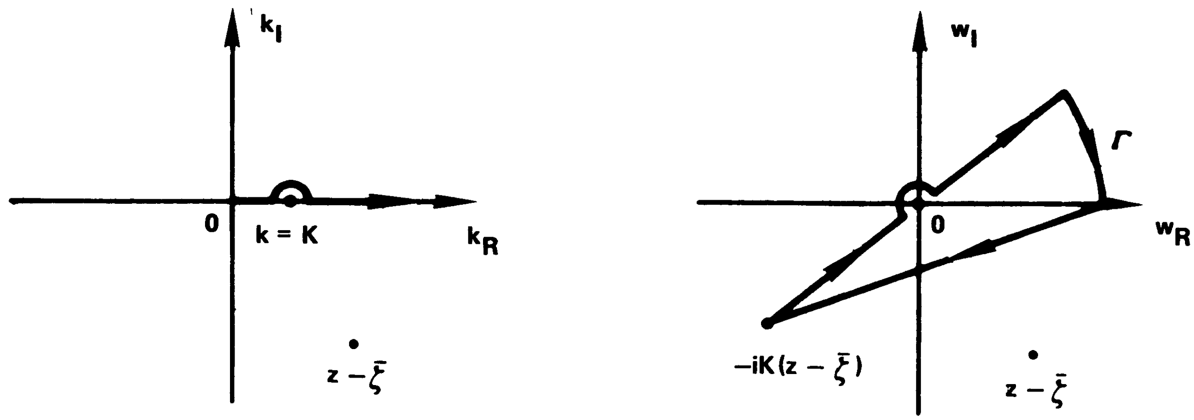

Figure 29 - Change of Integral Path when $\mathrm{Re}\,(z-\bar{\zeta}) > 0$

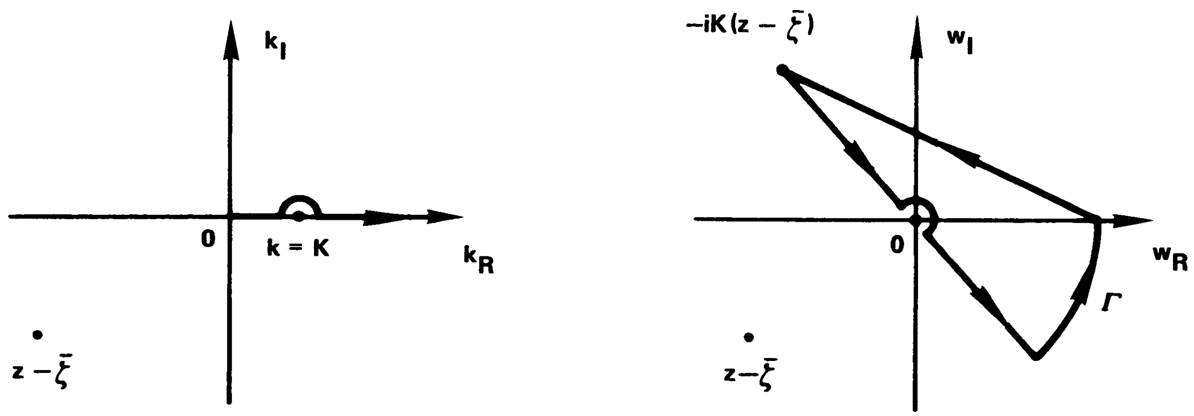

Figure 30 - Change of Integral Path when $\mathrm{Re}\,(z-\bar{\zeta}) < 0$

When $x-\xi > 0$ (Figure 29)

$$\int_{0 \atop \frown}^{\infty} \frac{e^{-ik(z-\bar{\zeta})}}{K-k} dk = -e^{-iK(z-\zeta)} \int_{-iK(z-\bar{\zeta})}^{\infty + i\infty} \frac{e^{-w}}{w} dw = e^{-iK(z-\bar{\zeta})} \left(\int_{\Gamma} + \int_{\infty}^{-iK(z-\bar{\zeta})} \frac{e^{-w}}{w} dw + 2\pi i \right)$$

$$= \left(\int_{\infty}^{-iK(z-\bar{\zeta})} \frac{e^{-w}}{w} dw + 2\pi i \right) e^{-iK(z-\bar{\zeta})} \qquad (67)$$

since $\int_{\Gamma = Re^{i\theta}}$ vanishes when we let $R \to \infty$.

Similarly, for $x - \xi < 0$, we can show (Figure 30) that

$$\int_{0 \atop \frown}^{\infty} \frac{e^{-ik(z-\bar{\zeta})}}{K-k} dk = -e^{-iK(z-\bar{\zeta})} \int_{-iK(z-\bar{\zeta})}^{\infty - i\infty} \frac{e^{-w}}{w} dw$$

$$= e^{-iK(z-\bar{\zeta})} \left(\int_{\Gamma} + \int_{\infty}^{-iK(z-\bar{\zeta})} \frac{e^{-w}}{w} dw \right) = e^{-iK(z-\bar{\zeta})} \int_{\infty}^{-iK(Z-\bar{\zeta})} \frac{e^{-w}}{w} dw \qquad (68)$$

Note that the singularity at $w = 0$ is outside of the closed path of the integration in this case; therefore, there is no residue value involved. The substitution of Equations (67) and (68) into (64) yields

$$⨍_{0}^{\infty} \frac{e^{-ik(z-\bar{\zeta})}}{K-k} dk = \int_{0 \atop \frown}^{\infty} \frac{e^{-ik(z-\bar{\zeta})}}{K-k} dk - i\pi e^{-iK(z-\bar{\zeta})}$$

$$= -e^{-iK(z-\bar{\zeta})} \int_{-iK(z-\bar{\zeta})}^{\infty} \frac{e^{-w}}{w} dw \pm i\pi e^{-iK(z-\bar{\zeta})} \text{ for } x-\xi \gtrless 0 \qquad (69)$$

We make use of the exponential integral which is defined by[11]

$$E_1(z) = \int_{z}^{\infty} \frac{e^{-t}}{t} dt \quad (\text{for } |\arg(z)| \leqslant \pi)$$

$$= -\gamma - \log z - \sum_{n=1}^{\infty} \frac{(-1)^n z^n}{n n!}$$

where $\gamma = 0.5772\cdots$ is the Euler constant, in Equation (69) to derive

$$\int_0^\infty \frac{e^{-ik(z-\bar{\zeta})}}{K-k}\,dk = -e^{-iK(z-\bar{\zeta})}E_1(-iK(z-\bar{\zeta})) \pm i\pi e^{-iK(z-\bar{\zeta})}$$

$$= e^{K(y+\eta)}\left\{\cos K(x-\xi) - i\sin K(x-\xi)\right\}\left[\left\{\gamma + \log r + \sum_{n=1}^{\infty}\frac{r^n \cos n\theta}{n\,n!}\right\} + i\left\{\theta + \sum_{n=1}^{\infty}\frac{r^n \sin n\theta}{nn!}\right\}\right] \quad (70)$$

where $r = K\left\{(x-\xi)^2 + (y+\eta)^2\right\}^{1/2}$ and $\theta = \tan^{-1}\dfrac{x-\xi}{-(y+\eta)}$

If we let

$$A(r,\theta) = \gamma + \log r + \sum_{n=1}^{\infty}\frac{r^n \cos n\theta}{n\,n!} \quad (71)$$

and

$$B(r,\theta) = \theta + \sum_{n=1}^{\infty}\frac{r^n \sin n\theta}{n\,n!} \quad (72)$$

we can separate Equation (70) into its real and imaginary parts

$$\int_0^\infty \frac{e^{k(y+\eta)}\cos k(x-\xi)}{K-k}\,dk = e^{K(y+\eta)}\left\{A(r,\theta)\cos K(x-\xi) + B(r,\theta)\sin K(x-\xi)\right\} \quad (73)$$

and

$$\int_0^\infty \frac{e^{k(y+\eta)}\sin k(x-\xi)}{K-k}\,dk = e^{K(y+\eta)}\left\{A(r,\theta)\sin K(x-\xi) - B(r,\theta)\cos K(x-\xi)\right\} \quad (74)$$

Exactly identical derivations as shown in Equations (73) and (74) can be applied for the integral

$$\int_0^{\infty} \frac{e^{-ik(z+\zeta)}}{K-k}\, dk$$

except that r and θ for this case are defined by

$$r = K\left\{(x+\xi)^2 + (y+\eta)^2\right\}^{1/2}$$

and

$$\theta = \tan^{-1} \frac{x+\xi}{-(y+\eta)}$$

REFERENCES

1. Potash, R., "Forced Oscillation of Two Rigidly Connected Cylinders on a Free Surface," M.S. Thesis, University of California, Berkeley (1967).

2. Ohkusu, M., "On the Heaving Motion of Two Circular Cylinders on the Surface of a Fluid," Reports of Research Institute of Applied Mechanics, Kyushu University (Japan) Vol. 17, No. 58 (1969).

3. Ohkusu, M., "On the Motion of Multihull Ships in Waves (I)," Reports of Research Institute of Applied Mechanics, Kyushu University (Japan) Vol. 18, No. 60 (1970).

4. Wang, S. and Wahab, R., "Heaving Oscillations of Twin Cylinders in a Free Surface," Journal of Ship Research, Vol. 15, No. 1 (1971).

5. de Jong, B., "The Hydrodynamic Coefficients of Two Paralleled Identical Cylinders Oscillating in the Free Surface," International Shipbuilding Progress Vol. 17, No. 196 (Dec 1970).

6. Ursell, F., "On the Heaving Motion of a Circular Cylinder on the Surface of a Fluid," Quarterly Journal of Mechanics and Applied Mathematics, Vol. 2, (1949).

7. Frank, W., "Oscillation of Cylinders in or below the Free Surface of Deep Fluids," NSRDC Report 2375, (Oct 1967).

8. Wehausen, J. V. and Laitone, E.V., "Surface Waves," Encyclopedia of Physics, Vol. 9, Springer-Verlag, Berlin, (1960).

9. Kellog, O. D., "Foundations of Potential Theory," Dover Publications, Inc., New York (1929).

10. John, F., "On the motion of Floating Bodies, Part II," Communication of Pure and Applied Mathematics, Vol. 3 (1950).

11. Abramowitz, M. and Stegun, I. A., "Handbook of Mathematical Functions," National Bureau of Standards, AMS 55, (1965).

INITIAL DISTRIBUTION

Copies	
1	NAVMAT (Code 0331)
9	NAVSEC 1 SEC 6110 1 SEC 6114D 3 SEC 6114H 2 SEC 6136 2 SEC 6111B
5	NAVSHIPS 3 SHIPS 2052 1 SHIPS 034 1 SHIPS 525
3	NAVORDSYSCOM 1 Aero & Hydro Br (Code RAAD-3) 1 Ship Instal & Des (Code SP-26) 1 Loads & Dyn Sec (Code RADD-22)
4	CHONR 1 Nav Analysis (Code 405) 1 Math Br (Code 432) 2 Fluid Dyn (Code 438)
1	ONR, New York
1	ONR, Pasadena
1	ONR, Chicago
1	ONR, Boston
1	ONR, London
1	CDR, USNOL, White Oak
2	DIR, USNRL (Code 5520) 1 Mr. Faires
1	CDR, USNWC, China Lake
1	CDR, NUR&DC, Pasadena
1	CDR, USNAVMISCEN, Point Mugu
1	DIR, Natl BuStand Attn: Dr. Schubauer
12	DDC

Copies	
1	DIR, APL, JHU, Silver Spring
1	DIR, Fluid Mech Lab, Columbia Univ
1	DIR, Fluid Mech Lab, Univ of Calif, Berkeley
1	Prof E.V. Laitone Aero Sci Div Univ of Calif Berkeley, Calif 94720
2	DIR, DL, SIT 1 Dr. C.H. Kim
3	McDonald-Douglas Aircraft, Aircraft Div, Long Beach, Calif 90801 1 Mr. A.M.O. Smith 1 Mr. J.L. Hess 1 Mr. J.P. Giesing
1	DIR, Scripps Inst of Oceano, Univ of Calif
1	DIR, Penn St Univ, Univ Pk
1	DIR, WHOI
1	Prof L. Ward Webb Inst of Nav Arch
2	DIR, Iowa Inst of Hydrau Research 1 Prof L. Landweber
2	DIR, St. Anthony Falls Hydrau Lab 1 Prof C.S. Song
5	Head, NAME, MIT, Cambridge 1 Prof Abkowitz 1 Prof Kerwin 1 Prof Newman 1 Prof Lewis 1 Prof Mandell
2	Inst of Mathematical Sci, NYU, New York 1 Dr. Stoker

Copies

3 Dept of Nav Architecture, Univ of Calif, Berkeley, Calif 94720
1 Prof J.V. Wehausen
1 Prof W.C. Webster
1 Prof J.R. Paulling

1 Prof Finn Michelsen, Dept of Nav Arch, Univ of Mich, Ann Arbor

2 Prof T.F. Ogilvie
Dept of Nav Arch, Univ of Mich, Ann Arbor

1 Prof Richard MacCamy, Carnegie Tech Pittsburgh 13

2 Hydro Lab, CIT, Pasadena
1 Prof T.Y. Wu

1 Dr. Hartley Pond, 14 Elliot Dr New London, Conn

1 Prof M. Van Dyke, Dept of Aero & Astro Stanford Univ, Palo Alto, Calif

1 Prof B.V. Korvin-Kourkovsky, P.O. Box 247, East Randolph Vt. 05041

2 Dept of Aero & Astro, MIT
1 Prof Widnall

1 DIR, Inst for Fluid Dyn & Appl Math Univ of Md

1 DIR, Hydrau Lab, Univ of Colorado

1 Pres, Oceanics, Inc
Technical Industrial Park
Plainview, N.Y.

1 Hydronautics, Inc., Pindell School Rd
Laurel, Md

2 Applied Mechanics Review
Editorial Office
Southwest Research Inst.
P.O. Box 28510
San Antonio, Texas 78228

CENTER DISTRIBUTION

Copies				
1	15			
	1	1506		
	1	1521		
	3	1524		
		1	Lin	
		1	Neal	
		1	Day	
	1	1528, Tejsen		
	4	154		
		1	1541	
		1	1542	
		1	1544	
	9	1552		
		1	McCarthy	
		1	Chang	
		1	Huang	
		1	Kerney	
		1	Langen	
		1	Peterson	
		1	Salvesen	
		1	Wang	
		1	Von Kerczek	
	8	156		
		1	1561.	
		38	1564	
			1	Monacella
			1	Wolff
			1	Sheridan
			15	Bedel
			20	Lee
		17	1568	
			1	Cox
			1	Zarnick
			15	Jones
	3	1572		
		1	Feldman	
		1	Gersten	
		1	Fein	
	3	1576		
		1	Smith	
		1	Russ	
		1	Livingston	

Copies		
2	1735	
	1	Genalis
1	174	
1	1802.3	
2	1843	
	1	Schot
	1	Oh
4	19	
	1	1903
	1	194
	1	1966, Liu

UNCLASSIFIED
Security Classification

DOCUMENT CONTROL DATA - R & D

(Security classification of title, body of abstract and indexing annotation must be entered when the overall report is classified)

1. ORIGINATING ACTIVITY (Corporate author) Naval Ship Research and Development Center Bethesda, Maryland 20034	2a. REPORT SECURITY CLASSIFICATION UNCLASSIFIED 2b. GROUP

3. REPORT TITLE

ADDED MASS AND DAMPING COEFFICIENTS OF HEAVING TWIN CYLINDERS IN A FREE SURFACE

4. DESCRIPTIVE NOTES (Type of report and inclusive dates)

5. AUTHOR(S) (First name, middle initial, last name)

C. M. Lee
H. Jones
J. W. Bedel

6. REPORT DATE August 1971	7a. TOTAL NO. OF PAGES 56	7b. NO. OF REFS 11

8a. CONTRACT OR GRANT NO. b. PROJECT NO. Subproject S-R009 01 01 Task 0100 c. d.	9a. ORIGINATOR'S REPORT NUMBER(S) 3695 9b. OTHER REPORT NO(S) (Any other numbers that may be assigned this report)

10. DISTRIBUTION STATEMENT

APPROVED FOR PUBLIC RELEASE: DISTRIBUTION UNLIMITED

11. SUPPLEMENTARY NOTES	12. SPONSORING MILITARY ACTIVITY Naval Ship Systems Command

13. ABSTRACT

A potential flow problem, dealing with twin horizontal cylinders of arbitrary cross sectional forms vertically oscillating in a free surface is investigated. An associated experiment is carried out for four different sets of twin cylinders. The results from the theory and the experiment are compared and are found in good agreement.

14 KEY WORDS	LINK A		LINK B		LINK C	
	ROLE	WT	ROLE	WT	ROLE	WT
Catamaran Motion						
Twin Cylinder Added Mass and Damping						
Free-Surface Effect						
Heaving Ship Near a Wall						

O. E. Browsery